Universität für Bodenkultur Wien
University of Natural Resources
and Life Sciences, Vienna

Master Thesis

Advanced 3D hydrogel culture of human mesenchymal stem cells

Submitted by

Michelle Lisa STEINDL, BSc

in the framework of the Master programme

Biotechnology

in partial fulfilment of the requirements for the academic degree

Diplom-Ingenieurin

Vienna, July 2022

Supervisor:

Univ.Prof. Dipl.-Chem. Dr. Cornelia Kasper
Institute of Cell and Tissue Culture Technologies
Department of Biotechnology

Affidavit

I hereby declare that I have authored this master thesis independently and that I have not used any assistance other than that which is permitted. The work contained herein is my own except where explicitly stated otherwise. All ideas taken in wording or in basic content from unpublished sources or from published literature are duly identified and cited, and the precise references included.

I further declare that this master thesis has not been submitted, in whole or in part, in the same or a similar form, to any other educational institution as part of the requirements for an academic degree.

I hereby confirm that I am familiar with the standards of Scientific Integrity and with the guidelines of Good Scientific Practice and that this work fully complies with these standards and guidelines.

Vienna, 16.07.2022 Michelle Lisa STEINDL *(manu propria)*

Acknowledgements

First and foremost, I would like to express my infinite gratitude to Prof. Dr. Cornelia Kasper for the opportunity to undertake my master thesis in her research group at the Institute of Cell and Tissue Culture Technologies at the University of Natural Resources and Applied Life Sciences. I would also like to thank her for inspiring my interest in the field of tissue engineering during her lectures throughout my master's degree.

I would like to show gratitude to my supervisor Dr. Dominik Egger whose immense expertise and plentiful experience were indispensable for finishing this thesis. I am deeply grateful for his permanent support and his suggestions for the finalization of the thesis. Despite the drawbacks in the laboratory, he always encouraged me and provided advice, assistance, and recommendations all along.

I would also like to acknowledge all other members of the research group for assisting me in learning the laboratory techniques, for their cooperativeness, and for providing a promotional and humorous working atmosphere. A special thank goes to Sabrina Nebel, Ilias Nikolits, and Sebastian Kreß for always providing advice and scientific input.

My gratitude also goes to Volker Lorber and Manfred Taschner of the company LifeTaq Analytics GmbH who always tried their best to further improve and develop the 3D cell cultivation system utilized in this project.

Finally, I must express my very profound gratitude to my family for facilitating my education and for their continuous encouragement and emotional support throughout my years of study.

Table of content

Abstract

Human mesenchymal stem cells (MSC) display various therapeutically relevant characteristics including an outstanding self-renewal ability, a high proliferation capacity as well as a multi-lineage differentiation potential. Due to their individual properties, MSC are considered as promising candidates for cell-based therapies in the field of regenerative medicine. Besides numerous clinical applications, the cells show auspicious potential to be used for the construction of in vitro models. The establishment of such constructs is important as they were shown to successfully contribute to studying disease mechanisms and can further be applied for drug screening, thus reducing animal testing.

In the present work, a hydrogel-based three-dimensional (3D) cell culture model with MSC in the Oli-UP 3D cell culture system should be established under physiologic conditions. Therefore, the growth behavior of primary adipose-derived MSC (adMSC) and the immortalized K5 iMSC line was validated during 3D expansion under normoxic and hypoxic conditions. It could be proven that the oxygen concentration is a crucial parameter significantly affecting cell proliferation, with both cell types displaying accelerated growth at low oxygen tension. It could further be identified that the immortalized cell line proliferates faster showing an enhanced migration potential compared to the primary adMSC. Moreover, the first important step towards a fully automated continuous 3D hydrogel expansion could be achieved in this work. However, for the successful establishment of the in vitro disease model in the Oli-UP 3D cell cultivation system, extensive effort needs to be raised to refine the device.

The findings of this work form the basis for further experiments toward the establishment of a fully automated 3D in vitro model having promising prospects to be effectively applied in scientific research in the future.

Kurzfassung

Humane mesenchymale Stammzellen (MSC) weisen zahlreiche therapeutisch relevante Eigenschaften auf, wobei sie über eine hervorragende Selbsterneuerungsfähigkeit, eine hohe Proliferationsfähigkeit sowie über ein multipotentes Differenzierungspotential verfügen. Aufgrund ihrer Charakteristika sind MSC vielversprechende Kandidaten für zellbasierte Therapien im Bereich der regenerativen Medizin. Neben zahlreichen klinischen Anwendungen können diese Zellen für die Schaffung von In-vitro-Modellen verwendet werden. Die Etablierung solcher Konstrukte ist wichtig, da sie zur Untersuchung von Krankheitsmechanismen sowie für das Arzneimittelscreening eingesetzt werden können, wodurch Tierversuche reduziert werden können.

In der vorliegenden Arbeit soll ein Hydrogel-basiertes dreidimensionales (3D) Zellkulturmodell mit MSC im Oli-UP 3D Zellkultursystem unter physiologischen Bedingungen etabliert werden. Dabei wurde das Wachstumsverhalten von primären aus Fettgewebe isolierten MSC (adMSC) und der immortalisierten Zelllinie K5 iMSC während der 3D Expansion unter normoxischen und hypoxischen Bedingungen validiert. Es konnte gezeigt werden, dass die Sauerstoffkonzentration die Zellproliferation maßgeblich beeinflusst, wobei beide Zelltypen erhöhtes Wachstum unter hypoxischen Bedingungen aufwiesen. Die immortalisierte Zelllinie zeigte, im Vergleich zu den primären adMSC, ein erhöhtes Proliferations- bzw. Migrationspotential. Darüber hinaus konnte in dieser Arbeit der erste wichtige Schritt hin zu einer vollautomatisierten kontinuierlichen 3D-Hydrogel-Expansion erreicht werden. Für die erfolgreiche Etablierung des In-vitro-Krankheitsmodells im Oli-UP 3D Zellkultivierungssystem ist jedoch eine grundlegende Adaptierung des Geräts erforderlich.

Die Ergebnisse dieser Arbeit bilden die Grundlage für die Etablierung des vollautomatisierten 3D In-vitro-Modells, welches zukünftig in der Forschung angewendet werden kann.

1 Introduction

1.1 Mesenchymal stem cells: identity and potential

1.1.1 Potency, properties, and isolation of mesenchymal stem cells

In general, there are numerous types of stem cells that originate from different parts of the human body or are formed at different times throughout life [1]. Those cells are classified according to their differentiation potential. Embryonic stem cells (ESC) isolated from embryonic tissue are pluripotent and can therefore differentiate into the cells of all three germ layers including the ectoderm, mesoderm, and endoderm. Induced pluripotent stem cells (iPSC) are obtained from differentiated somatic cells after they have been genetically reprogrammed by overexpression of particular transcription factors. As their name states, those cells are also pluripotent having the capacity to give rise to cells of all tissue types [2]. Pluripotent stem cells do normally not exist in adult organisms, whereas adult stem cells, also referred to as somatic stem cells, can be isolated from various specific tissues in the organism such as fat, skin, bone marrow, blood, or skeletal muscle. Those cells are either multipotent differentiating into multiple cell types within a particular lineage, or unipotent forming only one cell type [2][3]. Although adult stem cells have a lower potency compared to ESC or iPSC, these cells are of utmost importance for research and clinical application. In contrast, the use of ESC and iPSC is restricted by cellular regulations and ethical concerns even though the therapeutic potential of these cells would be highly beneficial. The majority of adult stem cells are present in the bone marrow with multipotent mesenchymal stem cells (MSC), also designated as mesenchymal stromal cells, among them [2][4].

As all types of stem cells, human MSC possess a high self-renewal ability meaning that the cells can divide indefinitely. Other characteristics are their high proliferation capacity, their capability to be expanded over several passages in vitro, and the ease of obtaining the cells from donors in large numbers. Moreover, those cells have the potential to differentiate into multiple cell lineages [3][5]. However, the actual properties of MSC can be highly diverse being affected by factors such as the tissue source, the isolation method, and even the medium composition [5]. Those facts make it quite difficult to define a uniform cell type for

MSC. In 2006, the International Society for Cellular Therapy defined a set of minimal criteria including markers and cell features for the identification and characterization of MSC [3][5]. According to this widely accepted approach, MSC have to possess a self-renewal ability, differentiate into adipogenic, chondrogenic, and osteogenic lineages, and express a distinctive set of surface markers. These markers comprise the clusters of differentiation (CD)73, CD90, and CD105, whereas CD14, CD34, CD45, and human leukocyte antigen-DR (HLA-DR) should be absent [5].

MSC have originally been identified in the bone marrow which has also been the prevailing source of MSC in humans in the past. However, the bone marrow contains a comparatively small number of MSC, and cell isolation is a painful procedure requiring general anesthesia [3][5][6]. In recent years, alternative sources for MSC have been discovered and it has been shown that those cells can be obtained from several other tissues in the human body including adipose tissue, dental tissues, skin and foreskin, salivary gland, limb buds, menstrual blood, and perinatal tissues [5]. By characterizing the MSC isolated from different sources, it was found that the cells differ in terms of collection procedure, cell quantity, immaturity, and cell profile [1].

Among the sources mentioned, umbilical cord tissue and adipose tissue are the most promising and relevant sources, whereas especially the latter one is ubiquitous and abundantly available. Furthermore, high numbers of cells, referred to as adipose-derived MSC (adMSC), can be easily isolated from adipose tissue which can be obtained using a minimally invasive procedure with little donor-site morbidity. Adipose tissue contains up to 3 % stem and progenitor cells among other cell types in its stromal vascular fraction [5]. The most relevant source for adMSC is the white, subcutaneous adipose tissue which is a surgical waste product. The cells are thereby typically isolated from the subcutaneous tissue of the abdomen, thigh, and arm [3][5]. As adMSC are ubiquitous and easily obtainable in large numbers, those cells are one of the most promising stem cell populations identified so far and have great potential to be implemented in the field of regenerative medicine. Nevertheless, it has to be considered that the functional characteristics of the adMSC and numbers of cells isolated differ greatly depending on the anatomical areas they were obtained from as well as on the donor characteristics such as age, gender, body mass index and disease history. Moreover, there are different isolation methods applied being either based on enzymatic

isolation or explant culture with no definition of a standardized procedure. Even small variance in those different harvesting procedures leads to high variation in quality, yield, and composition of the isolated cell population. These findings reveal that adMSC have a quite heterogeneous character influenced by numerous factors [1][3][5].

1.1.2 Characterization of adipose-derived mesenchymal stem cells

AdMSC are fibroblast-like cells that generally show similar properties to MSC isolated from other tissues and are identified by a set of criteria. AdMSC are typically characterized by their plastic-adherent growth showing a spindle-shaped morphology, their high expansion rates, and their cell surface CD antigen profile analyzed by flow cytometry. However, to date, it has not been possible to determine a single surface marker that alone identifies a cell as an adMSC which is why a set of markers has been defined that characterizes this cell type. However, the data reported in the literature are quite diverse regarding the definition of the marker antigens. The reasons lie in the heterogeneity of adMSC populations isolated as the cell features are affected by donor characteristics, the type and location of fat tissue used as well as by the different isolation and cultivation methods applied with some surface antigens being for instance only present under certain cultivation conditions [6][7]. AdMSC are mainly identified by the expression of the distinctive surface markers CD13, CD29, CD44, CD49b, CD90, and CD105, whereas they should be negative for CD14, CD31, CD45, and CD144 [6]. Although adMSC share common MSC characteristics, they clearly differ in terms of population number, proliferative capability and differentiation abilities [1].

AdMSC are additionally characterized by their differentiation potential into lineage-specific terminally differentiated cells what is a general hallmark of MSC. In vitro differentiation is generally induced by supplying the multipotent cells with specialized selective media supplemented with lineage-specific components. The differentiation can finally be evaluated by staining the cells with solutions specific to the respective cell type. All MSC, including adMSC, should be capable of efficiently differentiating into adipocytes, osteoblasts, and chondrocytes, which are all cells of mesodermal origin [3][6]. In addition, the differentiation into myocytes, also of mesodermal origin, was confirmed in many studies [8][9]. It has also been demonstrated in several trials that adMSC, which are of mesodermal origin, even have the capacity to differentiate along ectodermal and endodermal lineages in vitro under certain

conditions [3]. According to literature, the cells can efficiently be differentiated into keratinocytes, hepatocytes, and beta islet cells [10][11][12]. It has also been reported that adMSC can successfully differentiate into vascular endothelial cells and interconnect with the vascular network despite this differentiation being assessed as relatively difficult [13]. Although controversial, some studies also revealed that adMSC show the potential to differentiate into neuronal and glial lineages of ectodermal origin [14]. Figure 1 gives an overview of the differentiation capacity of adMSC. It can again be asserted that there are variations in the differentiation potential of adMSC depending on the source of tissue they were obtained from as well as on the media composition and serum supplementation during expansion and differentiation [3][6].

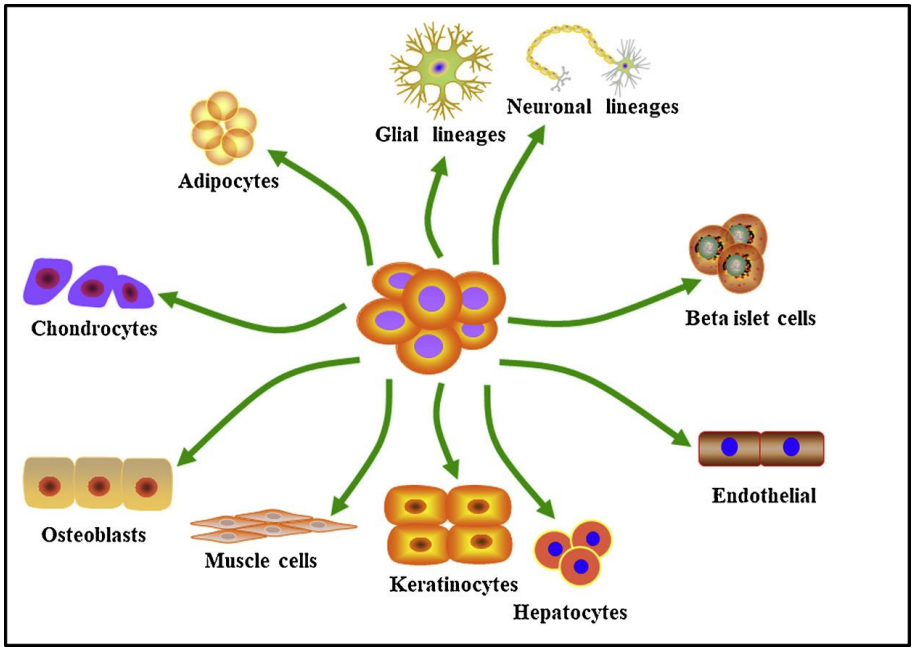

Figure 1: Differentiation potential of adMSC into distinct cell types. Besides the highly characteristic differentiation capacity into adipocytes, chondrocytes, and osteoblasts, studies also confirm the differentiation along ectodermal and endodermal lineages in vitro [3].

1.1.3 Therapeutic potential of adipose-derived mesenchymal stem cells

Due to their individual and therapeutically relevant characteristics comprising a high self-renewal capacity as well as the multi-lineage differentiation potential, MSC are promising candidates for cell-based therapies in the field of regenerative medicine. Cell-based therapies comprise cell isolation, in vitro expansion, and the subsequent application. In comparison to conventional biopharmaceuticals where cells are used to produce a certain drug, the cells

themselves, cellular products, or a tissue-engineered cell-matrix construct can be the final product in stem cell-based therapies [15].

The field of research is rapidly increasing as the cells may provide therapeutic solutions for numerous diseases. As one of the most promising stem cell populations identified so far, adMSC are under investigation for the treatment of a variety of human diseases. One property that makes adMSC a promising therapeutic tool is their outstanding tissue regeneration potential, comprising the ability to efficiently replace, repair, or regenerate dead or damaged cells [3]. The field of tissue engineering is especially important as organ failure and tissue loss are challenging health issues with the availability of organs for transplantation being strongly limited and conventional artificial implants being restricted in their application [16].

The tissue regeneration potential is based on different mechanisms of action including a direct pro-regenerative capacity with the cells differentiating into specific cell types. Thereby, damaged cell populations can be replaced when engrafting the cells in injured tissues in vivo. Moreover, it is reported that adMSC act primarily through paracrine mechanisms and cell-to-cell signalling by secreting particularly cytokines and growth factors [6]. The multipotent cells are attracted to injured tissues by chemotactic signals and subsequently promote tissue regeneration by restoring the common tissue function or at least reducing the damage caused by injury or disease. After migrating to the injured site, adMSC can differentiate into several cell lineages, while cell regeneration and proliferation are stimulated through the secretion of soluble factors [6][17]. The cytokine profile comprises soluble factors such as vascular endothelial growth factor (VEGF), granulocyte/macrophage colony-stimulating factor (GM-CSF), stromal-derived factor 1-alpha (SDF-1α), hepatocyte growth factor (HGF), transforming growth factor beta (TGF-β), fibroblast growth factor 2 (FGF-2) and nerve growth factor (NGF) [6]. These mediators are responsible for the beneficial therapeutic effects adMSC exert. It has for example been shown that adMSC exhibit a neuroprotective activity and support the regeneration of central nervous system cells [18]. Moreover, studies demonstrate that adMSC have great potential in bone regeneration which can be attributed to their ability to differentiate into osteoblasts and chondrocytes [3][19]. Research exhibited that the multipotent cells can efficiently form new bone and cure large calvarial defects [20]. Additionally, adMSC have been demonstrated to be effective in pathologic wound healing as

they secrete various growth factors and cytokines that are involved in angiogenesis and neovascularization [3][21].

Another important fact is that adMSC show immunomodulatory effects having the ability to regulate the local and systemic immune response directly or indirectly by interfering with the cells of the innate and adaptive immune system. Depending on the physiological conditions, the microenvironment, the oxygen concentration, and the stimulation by inflammatory factors, adMSC show both, immunosuppressive as well as pro-inflammatory activity [17]. MSC generally express a high number of cell surface receptors called Toll-like receptors (TLR), whereas a connection between the type of receptors present and the direction of the immune response can be observed. TLR are stimulated by paracrine factors such as inflammatory cytokines and interleukins circulating in the microenvironment. It generally applies that, cells activated via TLR4 receptors show pro-inflammatory activity and are referred to as MSC1 cells, whereas so-called MSC2 cells have anti-inflammatory or immunosuppressive activity and are stimulated through TLR3 receptors [17][22]. The activation of TLR results in the mobilization of innate immune cells such as neutrophils, macrophages, dendritic cells, and natural killer cells as well as of adaptive immune cells including T lymphocytes and B lymphocytes. The immunomodulatory activity can thereby be mediated by direct cell-to-cell interaction between the adMSC and the immune cells or through a paracrine signalling mechanism. In this paracrine route, the immune regulation is based on the secretion of soluble molecules such as cytokines, chemokines, growth factors, exosomes, and extracellular vesicles that affect the inflammatory process, whereas the exact mechanisms behind are not fully understood to date [17].

With the mechanisms of action of adMSC being investigated and revealed, those cells gain ever more therapeutic potential in many clinical settings. Applications are currently being investigated in numerous clinical trials in nearly every field of health and medical research, whereas adMSC show promising characteristics for the treatment of autoimmune diseases, inflammatory or immunological disorders, and for general tissue repair [7][17]. According to the frequency of clinical trials by November 2021, adMSC are especially under investigation for the treatment of diseases concerning the digestive system, connective tissue, skin, central nervous system as well as musculoskeletal and cardiovascular disorders [23]. Besides those clinical applications, the cells also show promising potential to be used for the construction

of in vitro disease models. Such cell constructs can be used for studying disease mechanisms, contribute to the understanding of the role and mechanisms of action of MSC in various regenerative processes, and can further be applied in drug screening approaches, thus reducing animal testing. The European Medicine Agency (EMA), as well as the Food and Drug Administration (FDA), recently integrated MSC as therapeutical products into the category of medicines establishing an adequate legal framework as well as a clearly defined jurisdiction. In Europe, the EMA designated MSC and their derivative products as Advanced Therapies Medicinal Products (ATMPs) regulated by Regulation 1394/2007 [17]. However, most clinical trials are still at an early stage and there are a lot of challenges to face. To ensure the safety and efficacy of stem cell-based therapies and to achieve reproducible treatment outcomes, it is vital to develop standardized methods for cell isolation, cultivation, proliferation, and differentiation to obtain homogenous cell populations. Moreover, the correlation between the therapeutic effectiveness and the variation of donor characteristics needs to be deeply explored [7][17].

In addition, the mechanisms underlying stem cell development including intercellular and intracellular signalling pathways need to be more precisely investigated and understood [16]. Another challenge remains the delivery of MSC into the body in case of a stem cell transplantation. Most studies report a direct local injection at the site of injury or a systematic intravenous injection of the cells. However, both strategies result in low MSC survival and clearance within a few hours after transplantation [24][25]. As an efficient MSC transplantation requires a large number of cells, multiple doses of MSC are usually needed to achieve clinical efficacy which is why an effective in vitro expansion comes into focus [25].

1.1.4 Establishment of a mesenchymal stem cell line

As highlighted in the previous section, primary multipotent adMSC show promising therapeutic potential for the treatment of numerous diseases. However, such therapeutic approaches suppose the disposability of defined MSC subpopulations what remains a challenge since the cellular properties are affected by various factors. Although primary MSC can be easily expanded in vitro, prolonged culture and passaging result in reduced proliferation rates, differentiation capacity and cellular senescence. Another consequence of extended cultivation is that chromosomal instabilities could appear leading to numerical

and/or structural chromosomal aberrations [26]. Hence, MSC of higher passages are less secure and potent and should not be used in trials or clinical practice. These facts result in the need for large numbers of primary MSC that should ideally be isolated from the same donor to avoid the results as well as the comparability and reproducibility of experiments being affected by donor variabilities. Consequently, the number and extent of trials that can be conducted with cells from the same donor are restricted by the cell numbers that can be obtained during the first few passages [26][27].

The establishment of an immortalized MSC cell line having similar cellular characteristics as primary MSC could help to manage all these challenges. Therefore, a human adMSC line was generated from primary cells obtained from fat tissue by the application of a novel technology that is based on the transduction of primary cells with a lentiviral gene library [26][27]. The expansion genes introduced are linked to characteristics such as development, cell cycle progression, self-renewal, suppression of senescence, and regulation of differentiation or maintenance of pluripotency. For the generation of clonal cell lines, primary adMSC were randomly transduced with the gene library composed of 33 different transgenes, after being further cultivated until colonies arose. After isolation and expansion of single colonies, the most suitable clone was selected based on the cell morphology, immunophenotype, and proliferation potential. The selected clone K5 iMSC was then comprehensively characterized, whereas the integrated genes were identified, and a set of cell culture experiments was conducted to compare the clone to the original primary MSC. The examination of the gene integration pattern indicated that the K5 iMSC clone was transduced with 12 expansion genes including genes accountable for stemness and maintenance of adult stem cells. The cell morphology of primary cells and immortalized K5 iMSC was generally similar, whereas both cell types showed a fibroblast-like, spindle-shaped morphology. However, some differences could be detected with the K5 iMSC displaying a shorter cell length and more rounded cell bodies. Moreover, the flattened areas observed in the cell bodies of the primary MSC were widely absent in the immortalized cell line [26]. Figure 2 depicts the differences in cell morphology regarding the primary MSC and the immortalized K5 iMSC.

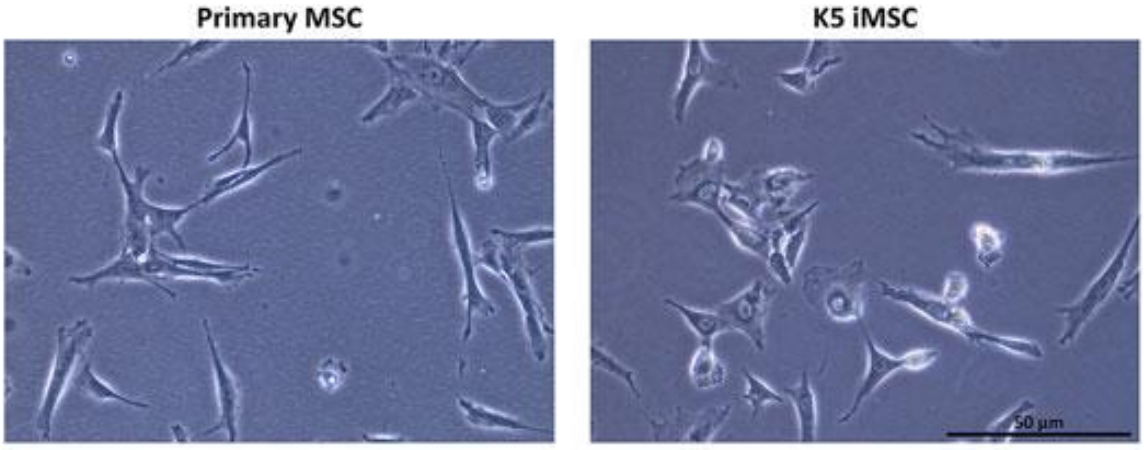

Figure 2: Cell morphology of primary MSC and the immortalized cell line K5 iMSC. Compared to the original primary cells, the K5 iMSC display a shorter cell length and more rounded cell bodies, whereas the flattened areas observed in the cell bodies of the primary MSC are widely absent [26].

The immunophenotype identified was equal to the original primary MSC with the expression of surface marker antigens being identical in both cell types. Regarding the proliferation potential, the K5 iMSC showed higher capacity compared to the original primary MSC. The immortalized cell line revealed a higher colony-forming unit potential and proliferated more quickly achieving a higher population doubling level within the observed subculture period. Furthermore, the K5 iMSC displayed an enhanced migration potential compared with the primary MSC in the monitored time frame. When exposed to the respective differentiation media, both cell types showed identical trilineage differentiation capacity. The cytogenetic analyses did not reveal any significant genetic instabilities or clonal aberrations for both, the primary MSC and the K5 iMSC. The findings reveal that the novel immortalization approach was successful and made it possible to generate the human adipose-derived K5 iMSC line showing even beneficial MSC characteristics resembling juvenile MSC or more potent MSC subpopulations [26].

1.2 Physiologic cultivation of MSC

For the therapeutic application of MSC, it is usually required to expand the cells ex vivo to reach higher cell numbers. However, the traditional two-dimensional (2D) cultivation of MSC on polystyrene tissue culture treated plastic surfaces, such as well-plates, petri dishes, or T-flasks, does not represent the physiologic environment of these cells [15]. It was shown in several studies that these static cultivation conditions could even alter characteristic stem cell properties leading to genetic instability or malignant transformation of MSC [28][29]. The

cells displayed low survival rates, altered surface marker profiles, and impaired differentiation capacities resulting in limited therapeutic success in clinical studies [30]. During the cultivation on 2D platforms, the cells lack fundamental natural microenvironmental characteristics such as physical and biochemical cell-cell and cell-matrix interactions, signalling via various molecules or gradients of nutrients, oxygen, and metabolic waste products [31].

Consequently, physiological cultivation conditions help to gain more reliable information about in vivo cell behavior and to better understand intercellular and cell-matrix interactions as the current understanding of many biological processes is largely based on studies conducted in 2D cell culture. Physiological in vitro cultivation conditions throughout the whole ex vivo expansion are crucial to obtaining cell populations with the desired therapeutic properties for applications in cell-based therapies [15][32]. It could be demonstrated that cells isolated, expanded, and eventually differentiated under conditions closely resembling the in vivo situation show even enhanced therapeutically relevant functions such as increased proliferation, higher viabilities, prolonged maintenance of stemness, and genetic stability [15][33-35]. Such physiological cultivation conditions mimicking the natural environment of the cells in vitro can be obtained by three-dimensional (3D), dynamic cultivation under hypoxic oxygen concentrations (see Figure 3). Besides those factors mentioned, various other chemical, biological and physical parameters need to be considered to generate an environment for the MSC that closely resembles the in vivo situation [15].

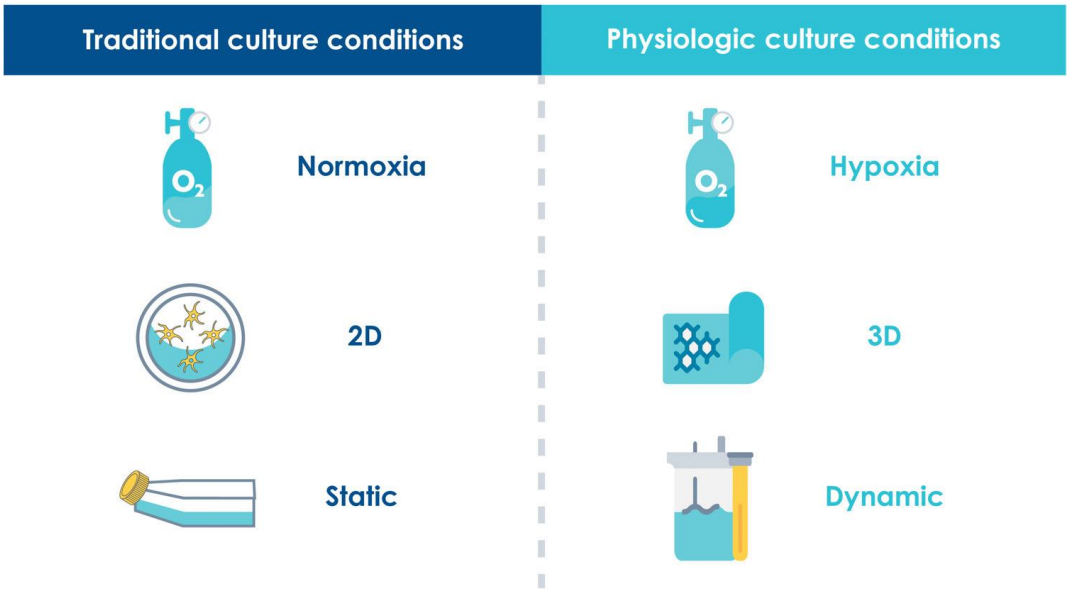

Figure 3: Comparison of traditional and physiologic cultivation conditions. While the traditional 2D static cultivation of MSC under ambient oxygen concentrations affects stem cell characteristics, the cultivation under physiologic conditions has beneficial effects on cellular therapeutically relevant functions. Cultivation conditions mimicking the natural environment of MSC in vitro comprise 3D dynamic cultivation under hypoxic oxygen concentrations [15].

1.2.1 From 2D to 3D cultivation

For the 3D expansion, MSC can either be cultivated scaffold-based on matrices where they get entrapped in pores of various biomaterials to achieve a spatial arrangement or in scaffold-free self-organized cellular aggregates referred to as spheroids building up their own extracellular matrix (ECM). An important approach of scaffold-based cultivation is the encapsulation of MSC in hydrogels for 3D physiologic cultivation [31][36].

The expansion of the cellular in vitro environment by a third dimension has a great impact on various cellular characteristics including cell morphology, shape, and organization, whereas the cell structure and function are further influenced by the mechanical forces acting between the cells and their surroundings. For the basic understanding of 3D MSC cultivation, it is important to know that those cells are naturally embedded in a complex and information-rich environment surrounded by an ECM that represents the structural basis for the respective tissue in the body and provides the fundamental basis for cell-cell and cell-matrix signalling interactions [37]. Figure 4 illustrates the main differences between standard 2D cell culture and 3D cell culture.

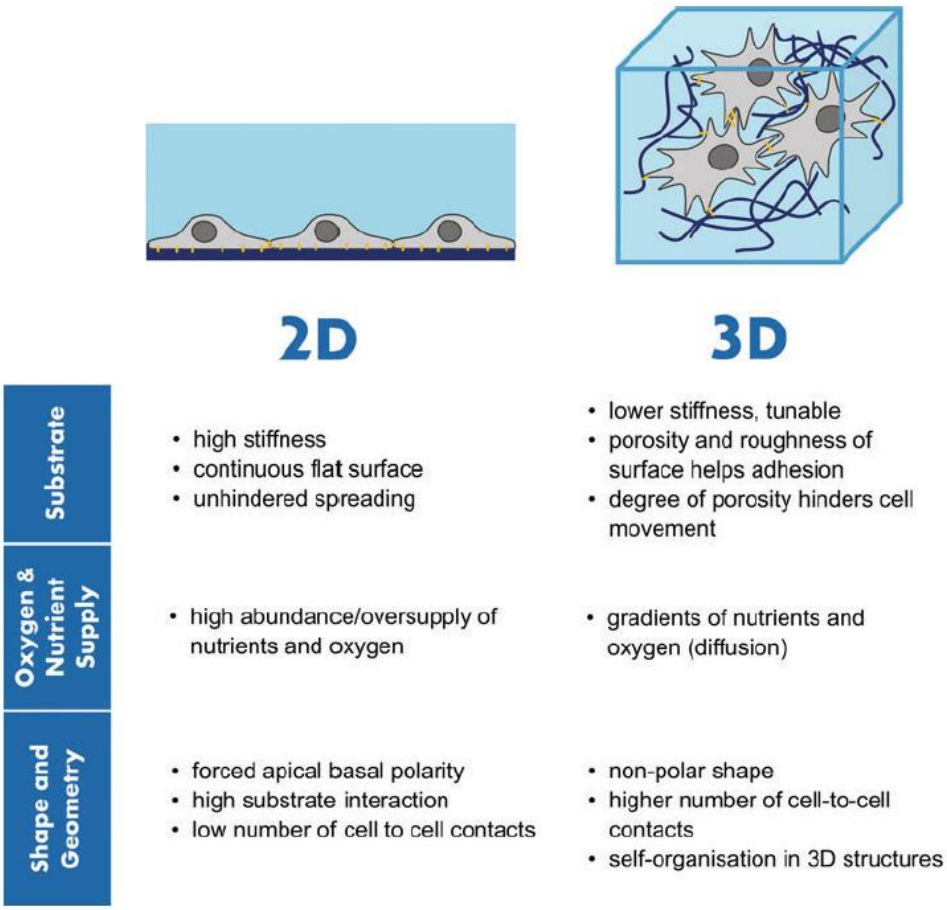

Figure 4: Differences between standard 2D cell culture and 3D cell culture. The illustration compares the cell shape (grey), the substrate (dark blue) and cell adhesion points (yellow). The main differences between 2D and 3D cell culture concern the composition of the substrate, the oxygen and nutrient supply as well as the cell shape and geometry [37].

The composition of the ECM is tissue-dependent, whereby the main components comprise structural proteins including collagen and glycosaminoglycans that offer binding sites for cell adhesion. These proteins additionally release bioactive molecules that regulate cell growth, differentiation, and disease progression. Cell-matrix interactions are mainly mediated by integrin cell surface receptors that span the cell membrane and bind to specific amino acid sequences found in various ECM proteins. Besides offering mechanical support for cells, the ECM is also involved in controlling the spatial distribution of nutrients, gases, and soluble effector molecules, thus regulating basic cellular processes. Based on this information, many different biomaterials with incorporated ECM components have been designed to mimic the natural MSC microenvironment [32][38].

1.2.1.1 Scaffold-based 3D cultivation

For the scaffold-based 3D cultivation of cells, various supportive structures referred to as scaffolds or matrices made of different materials have been developed in recent years. The so-called biomaterials have been designed to cover a wide range of physical, chemical, and mechanical properties and provide an artificial extracellular microenvironment for the physiologic cultivation of MSC. In the field of tissue engineering, those 3D biomaterials are constructed to mimic the structural and biochemical functions of the natural ECM supporting the cells until they build up their own ECM. The cellular behavior is thereby regulated by the properties and architecture of the scaffolds including mechanical strength, porosity, pore size, and shape as well as interconnectivity. Moreover, the materials should possess biocompatible and bioactive characteristics to promote cell adhesion, proliferation, migration, and differentiation. Surface characteristics such as surface topography and chemistry thereby determine the scope of cell attachment and cellular spreading on the surface of the biomaterial. The biodegradability of the material is also crucial as different applications in tissue engineering require different degradation rates depending on the tissue formation process. This wide range of biomaterial features allows for an individual selection of the material for a scaffold depending on the tissue to be regenerated [16][39].

The three main classes of materials used in tissue regeneration are natural and synthetic polymers, ceramics as well as ECM-based biomaterials. Synthetic polymers are advantageous as they can be designed with a high degree of variation regarding the architecture as well as the physicochemical and mechanical properties and can therefore individually be constructed for the injured tissue. Examples of frequently used biodegradable synthetic polymers are aliphatic polyesters such as polylactic acid, polyglycolic acid, and the copolymer polylactic-co-glycolic acid. In contrast, natural polymers are derived from polysaccharides and proteins showing a high biodegradability and biocompatibility, whilst closely mimicking the natural ECM. Commonly used polysaccharide-based natural polymers include alginate and hyaluronic acid, whereas collagen, gelatine, and silk are frequently used proteins. Bioceramics are classified into nearly inert, bioactive, and resorbable ceramics showing great osteoconductivity and osteoinductivity, thus having promising potential to be used in bone regeneration. The most frequently used ceramics in this field are hydroxyapatite, calcium

phosphates, and tri-calcium phosphate each comprising chemical compositions, surface topographies, and conductivities similar to natural bone. ECM-based biomaterials are obtained from different decellularized ECM tissues, thus mimicking the native cellular environment closest as the micro- and macrostructure, the structural integrity, and the complex composition are retained during the decellularization process. The application of ECM-based biomaterials is restricted by several limitations such as donor shortage, although the scaffold material can also be derived from in vitro cultured cells [39].

1.2.1.2 Scaffold-free 3D cultivation

For the 3D MSC cultivation in spheroids, various techniques for the in vitro cell aggregate formation from a single cell suspension are available, each one having advantages and disadvantages while having the request to be robust and reproducible. The fabrication methods include for instance the traditional hanging drop technique, the use of low attachment microplates or structured microwells, and centrifugal aggregation techniques. The production technique has to be individually chosen for the respective application and requirements. Spheroid cultivation of MSC provides an environment for improved intercellular interactions with the cells forming their own ECM. Thereby, the cell-adhesion proteins cadherin and integrin contribute to the formation of an adhesive network and are further involved in cell signaling pathways [31][40]. The cultivation of MSC in self-assembled 3D aggregates was shown to retain the cellular biological functions and to have beneficial effects on the differentiation potential, the maintenance of stemness, and the cell survival observing delayed replicative senescence [41]. Moreover, MSC organized in a spheroid exhibit increased angiogenic, anti-inflammatory as well as immunomodulatory potential compared to cells cultured in 2D [41][42][43]. Taken together, this scaffold-free cultivation approach improves the therapeutic properties of MSC resulting in enhanced tissue regenerative effects. Besides the application of MSC aggregate cultivation in the field of tissue engineering, 3D cell spheroid-based in vitro models are used to investigate the cellular behavior under 3D conditions that mimic the physiologic environment [31][40].

1.2.1.3 3D cultivation in hydrogels

One of the most promising methods for scaffold-based 3D adMSC expansion is the cultivation in hydrogels [44]. Hydrogels are soft materials composed of natural or synthetic polymers forming porous networks that ingest large amounts of water. The biochemical, physical, and mechanical properties of hydrogels can be individually designed to mimic the in vivo microenvironment of MSC. Hydrogel features such as biodegradability, biocompatibility, mechanical strength, and porosity are adjustable and crucial for the extent of MSC proliferation and differentiation. By the individual selection of polymer materials and gelation methods, hydrogels for distinct applications in the field of regenerative medicine can be created. In general, hydrogels can be made of various natural or synthetic polymers by non-covalent or covalent crosslinking with the fabrication technique depending on the materials used (see Figure 5). Examples of naturally derived macromolecules are fibrin, hyaluronic acid, collagen type I, and alginate, whereas commonly used synthetic polymers comprise polyethylene glycol and polyacrylamide. Hydrogel networks generated from naturally derived macromolecules are generally established through non-covalent crosslinking by specific protein-protein interactions and non-specific charge-charge interactions. Those non-covalent interactions include ionic, electrostatic, and hydrophobic interactions, crystallization, or hydrogen bonding. Anionic alginate polymers can for example interact with divalent calcium cations to generate a hydrogel network. In comparison, synthetic polymer-based hydrogels are generated by covalent reactions such as amide formation and different cycloadditions, whereas the resulting networks are established by polymerization of monomers in a chain-growth manner or crosslinkers in a step-growth manner. The formation of the hydrogel network is based on the chemical reactions between the functional groups of different precursor molecules. Besides covalent or non-covalent crosslinking approaches, photopolymerization of (meth)acrylated precursors with ultraviolet (UV) or visible light is a widely used synthetic strategy for the preparation of hydrogels [38][44].

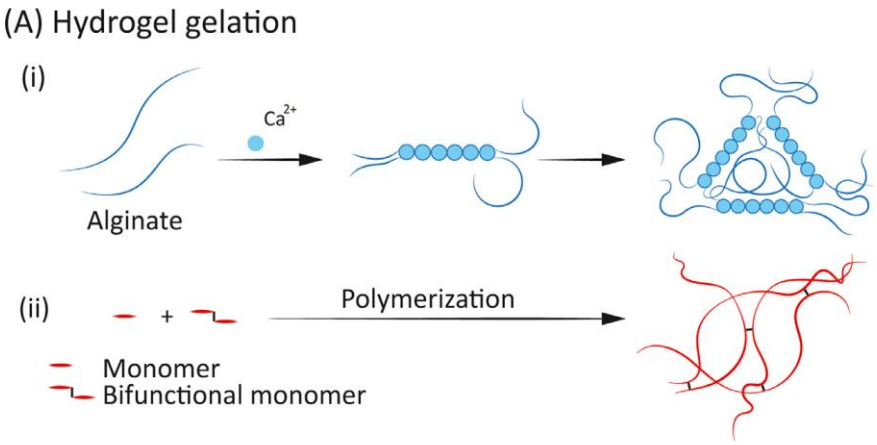

Figure 5: Schematic overview of methods for hydrogel gelation depending on the used polymers. (i) Gelation of natural alginate-based hydrogels through non-covalent crosslinking by non-specific charge-charge interactions with calcium cations, (ii) Hydrogel network generation from synthetic polymers through the polymerization of monomers via covalent bonds [38].

The mechanical features of hydrogels are determined by the crosslinking density, whereas the dynamic properties, responsible for the viscoelasticity and plasticity of the network, are controlled by the dynamics of crosslinking. The material properties of hydrogels can additionally be adapted by functionalizing the networks with specific biochemical and biophysical cues. These modifications can promote MSC proliferation and maintain regenerative properties during in vitro expansion, improve cell survival, retention, and engraftment in vivo and alter the MSC secretory profile. The binding of peptides for instance enhances cell adhesion, whereas growth factors and cytokines promote cell proliferation. Moreover, the mechanical features of hydrogels can be spatiotemporally regulated by integrating degradable sites into the hydrogel networks. Hydrogel degradation is commonly directed by photodegradable crosslinkers, enzymatic degradation of peptides, or redox-sensitive disulfide bonds [25][38].

Hydrogels can generally be used for the 2D cultivation of MSC on hydrogel surfaces, for the semi 2D cultivation inside hydrogel pores, or for the 3D cultivation of cells embedded within hydrogel networks. The cells are thereby either be mixed with the hydrogel solution before the gelation process or seeded onto the hydrogels after the crosslinking procedure [38].

Within the scope of this thesis, a gelatin-methacryloyl (GelMA) based hydrogel was used for the 3D in vitro cultivation of adMSC. GelMA is a semi-synthetic hydrogel that is constructed by derivatizing the natural polymer gelatin with methacrylic anhydride leading to the modification of lysine and hydroxyl residues with methacrylamide and methacrylate side

groups. This versatile hydrogel combines the utilization of the biological properties of gelatin with the individual adjustment of the mechanical features of the hydrogel network. The macromolecule gelatin retains many of its characteristics throughout the derivatization process including thermoreversible physical crosslinking and the availability of integrin-binding sequences as well as metalloprotease digestion sites. Therefore, the GelMA hydrogel provides an ideal biological environment for the cultivation of adMSC, supporting their adhesion, growth, and proliferation. The modification of gelatin with methacryloyl groups makes it possible to covalently crosslink the hydrogel together with a photoinitiator by exposure to UV light. The possibility of photo-crosslinking confers the hydrogel stability at a physiological temperature [45].

GelMA generally offers a wide range of adjustable parameters for the design of hydrogel networks providing the required stiffness and pore architectures. The mechanical properties of the GelMA hydrogel can individually be adapted depending on the gel strength of the chosen gelatin molecule, the hydrogel concentration, and the crosslinking density determined by the degree of functionalization (DoF) obtained after derivatization and the UV crosslinking conditions [36][45]. Thereby, a higher UV intensity or light exposure time resulted in increased stiffness of the gel, while the cell viability decreased and reduced cell spreading could be observed [45]. Consequently, the cellular behavior as well as the cell fate are directly related to the stiffness of the hydrogel network. The GelMA toolbox in Figure 6 provides an overview of the features that can be adjusted to reach the desired hydrogel properties required for the 3D cultivation of the cell type of interest. Moreover, the toolbox depicts the dependencies between the parameters and can be utilized to investigate the influence of alterations in the microenvironment on cell fate [36][45].

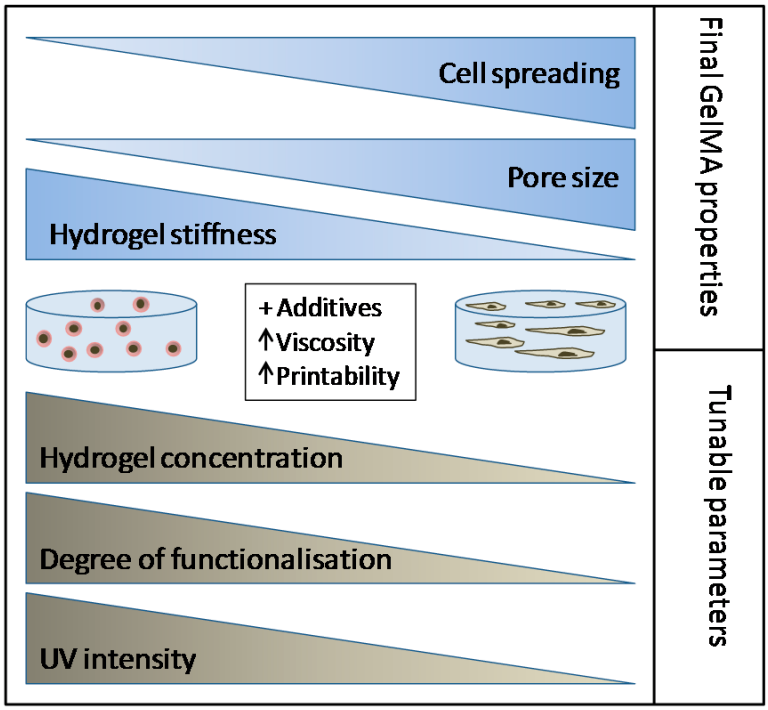

Figure 6: GelMA toolbox providing an overview of tunable parameters for reaching the desired hydrogel properties. By individually adjusting the hydrogel concentration, DoF, and UV intensity the GelMA properties can be adapted for the 3D cultivation of the cell type of interest [45].

Pepelanova et al. showed that for the 3D expansion of adMSC, a low GelMA concentration, as well as a low UV dosage, are beneficial for the provision of a cell promoting microenvironment supporting cell adhesion, spreading, and proliferation. Under these cultivation conditions, adMSC displayed their typical morphology and a high degree of viability. Besides the possibility of individually tuning the mentioned parameters, GelMA generally appears transparent after crosslinking facilitating microscopic analysis, and shows a high biocompatibility and degradability, while being rather cheap. Due to these individual characteristics, the hydrogel has been widely used for the 3D cultivation of cells as well as in tissue engineering approaches [45].

For the 3D cultivation of adMSC, a commercially available, photocrosslinkable GelMA-based hydrogel (LunaGel™ - Gelomics, Australia) was used used in the course of this thesis. The hydrogel is based on chemically modified pharmaceutical grade bovine bone gelatin containing different connective tissue glycoproteins and proteoglycans as well as the proteins collagen type I, III, IV, and V. The hydrogel supports cell attachment, proliferation, differentiation, migration as well as proteolytic degradation by providing a cell-instructive bioactivity similar to natural ECMs. LunaGel™ has a stiffness of 0-6.5 kPa that can individually be adjusted via the photocrosslinking technology by controlling the duration of light

exposure. The individually required physicochemical properties can consequently be controlled by the UV light intensity determining the matrix porosity and stiffness. For the formation of 3D cell culture models, the freeze-dried photoinitiator needs to be reconstituted in PBS. For casting the gel, equal amounts of photoinitiator and LunaGel™ are mixed with the resulting solution being photocrosslinked in the Luna Crosslinker™ [46].

1.2.2 Importance of hypoxic cultivation conditions

Another crucial microenvironmental parameter for the physiologic cultivation of adMSC is the oxygen concentration, which significantly affects cell behavior and physiology during cell cultivation. Depending on the tissue type, the metabolic activity of the corresponding cells, and the extent of vascularization, the average oxygen concentration in human tissues varies between 1 % and 15 %, with the latter one corresponding to the alveolar oxygen tension [15]. Consequently, the common so-called normoxic oxygen concentration of 21 % that prevails during conventional in vitro cell culture does not correspond to the natural in vivo environment of MSC. The cells show improved characteristics resulting in an enhanced therapeutic potential, under oxygen conditions much lower than the ambient concentrations [15][25]. Expansion of MSC under hypoxic (<21 %) oxygen concentrations leads to an elevated expression of growth factors, anti-apoptotic factors, pro-angiogenic and anti-inflammatory factors [47][48]. Moreover, it could be observed that MSCs from different sources showed an increased biological activity of extracellular vesicles, enhanced proliferation rates as well as an improved self-renewal capacity [49][50][51]. The reduction in oxygen tension additionally supports MSC to maintain their stemness and an undifferentiated cell phenotype leading to a prolonged genetic stability [52]. For adMSC, it was revealed that the concentration of the hypoxia-inducible transcription factor HIF-1a stabilized starting from an oxygen concentration of 7.5 % meaning that expansion at oxygen levels below this value has biological effects on these cells [53].

The control of the oxygen tension during the traditional 2D cultivation of MSC on plastic surfaces is relatively easy, whereas the achievement of hypoxic conditions in 3D cell cultures is quite challenging. During 2D cultivation, the oxygen must diffuse from the ambient air into the cell culture medium until it finally reaches the surface of the cell culture vessel. However, the oxygen diffusion inside a 3D cell construct is more complex with the cells in the outer

layers being well supplied consuming a large amount of the provided oxygen, whilst the ones in the core may not be supplied at all. However, the application of specific cell densities and construct sizes as well as dynamic cultivation conditions can help to reach controlled hypoxic oxygen concentrations [15].

1.3 3D dynamic cell cultivation systems

Besides the cultivation of MSC in a 3D environment under hypoxic oxygen concentrations, dynamic cultivation conditions are beneficial for the in vitro expansion of the cells. For the large-scale expansion of MSC, dynamic automated bioreactor systems are essential to establish an environment in which cells can be cultured with high consistency, reproducibility, and quality. Controlled culture parameters are required to obtain clinically relevant cell numbers with the cells showing the desired therapeutic properties to be further applied in cell-based therapies or to serve as in vitro models. These parameters comprise standard settings such as temperature, oxygen, carbon dioxide, and pH, whereas other important factors affecting cellular characteristics are fluid shear forces, media supply, and the choice of a suitable scaffold. Shear stress can for instance provoke spontaneous differentiation of MSC during cultivation. Therefore, the tight control of mechanical forces, such as shear stress that is inherently present in dynamic systems, is crucial to generating a physiologic environment as they greatly affect MSC properties [15][40]. The dynamic 3D cultivation is also beneficial concerning the continuous supply of cells with nutrients and oxygen as well as the removal of waste products. Continuous perfusion during cell expansion can contribute to enhanced consistency as metabolic products can be actively discharged, while the molecular composition of the medium remains constant [54].

It could be demonstrated in various studies that the MSC cultivation in dynamic bioreactor systems has a beneficial impact on the cellular properties resulting in enhanced therapeutic features [15][48-50]. Although MSC are sensitive to shear forces and the geometry of the bioreactor bed, an up to 2-fold higher cell proliferation could be observed during the 3D expansion in different bioreactors. Moreover, in terms of immunomodulatory and anti-inflammatory effects, an increased secretion of cytokines and chemokines could be detected during the dynamic MSC expansion. MSC cultured in dynamic systems additionally showed to maintain their stemness despite being expanded to large cell numbers in vitro [15].

1.3.1 Bioreactors suitable for the cultivation of hydrogels

For the cultivation of MSC embedded in hydrogels, several dynamic bioreactor systems have been developed and studied for successful in vitro cell expansion. The designed bioreactors should be advantageous over the traditional flask-based cell expansion in terms of traceability, staff workload, and costs. As the cultivation of the adherent adMSC requires a large surface area, the bioreactors should ideally provide a high surface-to-volume ratio, allowing for large-scale expansion with minimal manipulation. Moreover, the bioreactor systems should optimally be closed devices integrating numerous cell processing and cell culture steps within a single closed environment [15][56]. The already established dynamic bioreactor systems comprise types such as rotating-wall vessels, rotating-bed bioreactor systems, spinner flasks, direct perfusion systems, and hollow-fiber devices. Thereby, spinner flasks or stirred tank reactors are frequently used for the MSC cultivation on microcarriers [54].

MSC were for instance successfully expanded in a bi-axial rotating bioreactor system using a hydrogel composed of poly (ethylene oxide terephthalate)-co-poly (butylene terephthalate) (PEOT/PBT). After nine days of cultivation, an approximately 1.5-fold increased proliferation was determined in comparison to the static cultivation of cells in a well plate. It could additionally be proved that the MSC maintained their stem cell characteristics throughout the expansion period [15][55].

Other hydrogel-based systems for the dynamic cultivation of human MSC are based on cell expansion in spinner flasks. Zhao et al. demonstrated the efficient large-scale cultivation of human MSC in macroporous gelatin microbeads using spinning bottles as culture vessels. Compared to the cells in static culture, the MSC expanded in the dynamic environment showed a 1.5-fold higher proliferation index and entered the exponential growth phase two days earlier. The proliferation index was determined by the number of dead cells and proliferative cells. Moreover, the cells retained their typical surface marker profile, multipotent differentiation potential, self-renewal capacity as well as a healthy karyotype throughout the dynamic expansion period of ten days [15][57].

The commercially available Quantum Cell Expansion System by Terumo BCT is a hollow-fiber bioreactor that is automated, GMP compliant and provides a functionally closed environment. The device represents a perfusion bioreactor system that has already been used for the expansion of MSC in the course of clinical applications. However, in this system, the cells are grown on a porous matrix instead of growing inside a 3D scaffold. Consequently, the Quantum system only provides a "pseudo-3D" environment for MSC expansion. AdMSC cultured in the dynamic bioreactor system displayed an expansion rate twice as high as during 2D static cell cultivation in T-flasks. Moreover, it could be demonstrated that the hollow-fiber bioreactor provides an environment for safe and robust cell cultivation as the adMSC retained their characteristic surface marker profile and differentiation capacity even after extensive expansion [15][56].

Although vast progress has already been made in developing hydrogel-based bioreactor systems for the 3D stem cell cultivation, most devices still require a high degree of manual handling making it challenging to use them on a routine basis or for the large-scale expansion of cells. Moreover, it remains a challenge to fully mimic the biochemical, physical, and mechanical properties of the native stem cell microenvironment [15][54]. To date, a defined gold standard for the 3D expansion of adMSC in hydrogels is still missing, with no bioreactor system being commercially available for the specific cultivation of cells embedded in hydrogels.

1.3.2 3D Oli-UP cell culture system

The Oli-UP 3D cell culture system is a device generated for the 3D hydrogel expansion of cells. This manual 3D cell-culture kit was developed by the company LifeTaq-Analytics (Tulln, Austria) and is based on vertical cell cultivation in bespoke casting molds. The cell-culture kit consists of various parts including scaffold holders, cultivation chambers, autoclavable boxes, supporting elements, and seeding plates that are all reusable and autoclavable. For pouring the hydrogels, the molds made of silicon referred to as scaffold holders are placed on the supporting elements and put down on the seeding plates in an autoclavable box horizontally. The hydrogel solution is then poured into the small ports of the scaffold holders, which hold a volume of 90-95 µL of hydrogel. After successful crosslinking, the scaffold holders with the gels containing the cells are transferred in a vertical position into the so-called cultivation

chambers placed in another type of autoclavable box. Those chambers are either made of silicone, polytetrafluoroethylene (PTFE), or polyetheretherketone (PEEK) and are filled with cell culture medium. For the vertical cell expansion, the whole autoclavable box is put into the incubator [58]. The composition of the whole 3D cell culture system is depicted in section 2.3.

The Oli-UP cell culture system should prospectively be used for the fully automated 3D expansion of cells in a standardized, physiologic environment under reproducible conditions. A possible future application is for example the generation of high throughput 3D in vitro models that can further be used for the investigation of cellular processes or drug screening.

1.4 Aims of the thesis

This master thesis project is part of a research project funded by the Austrian Research Promotion Agency (FFG) in the “FFG Bridge” program. The project consortium consists of the BOKU Vienna, the IMC Krems, and the company LifeTaq-Analytics. The overall aim of this project is the development of an optogenetic MSC cell line from the immortalized K5 iMSC line for the precise regulation of immunomodulatory factors. The cell line should be validated under physiological conditions and should finally be used as an in vitro disease model. The establishment of such disease models is important as they contribute to the understanding of the role and mechanisms of action of MSC in various regenerative processes and they can further be applied for drug screening, thus reducing animal testing.

The whole project is divided into six work packages, whereas this thesis deals with work package five. The aim of this work package is the construction of a hydrogel-based 3D cell culture model with MSC in the Oli-UP 3D cell culture system. The 3D cultivation in the Oli-UP system is intended to provide physiological cultivation conditions that mimic the native environment of the cells so that they behave more like in vivo. Before starting the actual cultivation of the cells in the Oli-UP 3D cell culture system, the device should be characterized by performing various tests. Thereby, a cytotoxicity testing of the cultivation chambers should be carried out as the materials of the commercially available chambers of the cell culture system are not fully medical-grade. Moreover, the evaporation rate during cultivation in the Oli-UP system should be evaluated and the cell growth of primary adMSC should be characterized. Finally, the growth behavior of primary adMSC and the immortalized K5 iMSC line should be validated and compared during the 3D expansion in the Oli-UP under normoxic and hypoxic conditions by using suitable tests. As the focus of the project is on the full automation of the 3D cell culture model, the feasibility of the continuous 3D expansion of cells while being embedded in hydrogel should also be evaluated.

2 Material and Methods

All sterile work was performed in a class II flow hood whereby all used equipment was sprayed and sterilized with 70 % ethanol before use. The used media and solutions were autoclaved or sterile filtered before. Detailed lists of the used materials, as well as descriptions of the routinely used standard procedures, are listed in the appendix. If not stated otherwise all procedures were conducted as described in the appendix.

The human adMSC used in the experiments of this work were isolated from different donors, all given written consent. The adMSC were isolated from donor tissue and cultivated in cell culture medium composed of α-MEM, 0.5 % (v/v) gentamycin, 2.5 % (v/v) human platelet lysate (hPL) and 1 U/mL heparin in an incubator at 37°C and 5 % CO_2. The cells were cryopreserved in α-MEM, 10 % hPL, and 10 % DMSO and stored in a liquid nitrogen tank. If not stated otherwise, the cells used in the different experiments were cultured in cell culture medium of the above-mentioned composition.

2.1 Characterization of the Oli-UP 3D cell culture system

Before starting the actual cultivation of the adMSC in the Oli-UP 3D cell culture system, the device was characterized by performing various tests.

2.1.1 Cytotoxicity testing of the cultivation chambers

The commercially available cultivation chambers of the Oli-UP 3D cell culture system are either made of silicone or PTFE. As those materials are not fully medical-grade, it was investigated whether they impair the growth or physiology of the stem cells. Toxic components could to wit leach from the materials of the cultivation chambers into the cell culture medium during cell expansion and could then interfere with the cells.

2.1.1.1 Cells and medium used for material testing procedure

For testing the materials of the cultivation chambers the immortalized human adipose-derived K5 iMSC line was used, which is hereinafter referred to as the adMSC K5 cell line. Within the scope of the experiment, the cell line adMSC K5 in passage 7 was cultured at 37°C, 5 % CO_2, and 21 % O_2. The cells were stored in the liquid nitrogen tank, thawed, and seeded on a T-75 flask. After expanding the cells for two passages in cell culture flasks, they were seeded on a 48-well plate for further analysis.

For the cultivation of the adMSC cell culture medium was used.

2.1.1.2 Experimental design

For the experiment, the cultivation chambers of both materials tested were placed in the autoclavable boxes of the Oli-UP 3D cell culture system and were filled with 1 mL cell culture medium each after steam sterilization in the autoclave. The boxes were then put into the incubator for different periods of time. The media were incubated and conditioned for 24 hours, 48 hours, and 120 hours, whereby five cultivation chambers of each material were filled with medium for each cultivation period. In addition, control medium was incubated in a 24-well plate for the same periods of time. Therefore, five wells per condition were filled with 1 mL cell culture medium each. All media were incubated at 37°C, 5 % CO_2, and 21 % O_2.

In parallel, adMSC K5 in passage 9 were detached, counted, and seeded in 36 wells of a 48-well plate at a seeding density of 4000 cells/cm^2. Based on the defined seeding density and the area of one well of the 48-well plate, the required cell suspension volume per well for seeding the cells in the plate was calculated. For the cultivation, all 36 wells of the 48-well plate were filled with 200 µL cell culture medium. The plate was incubated at 37°C, 5 % CO_2, and 21 % O_2 for 24 hours. After 24 hours medium was changed, whereby the conditioned and control media were used according to the scheme in Figure 7.

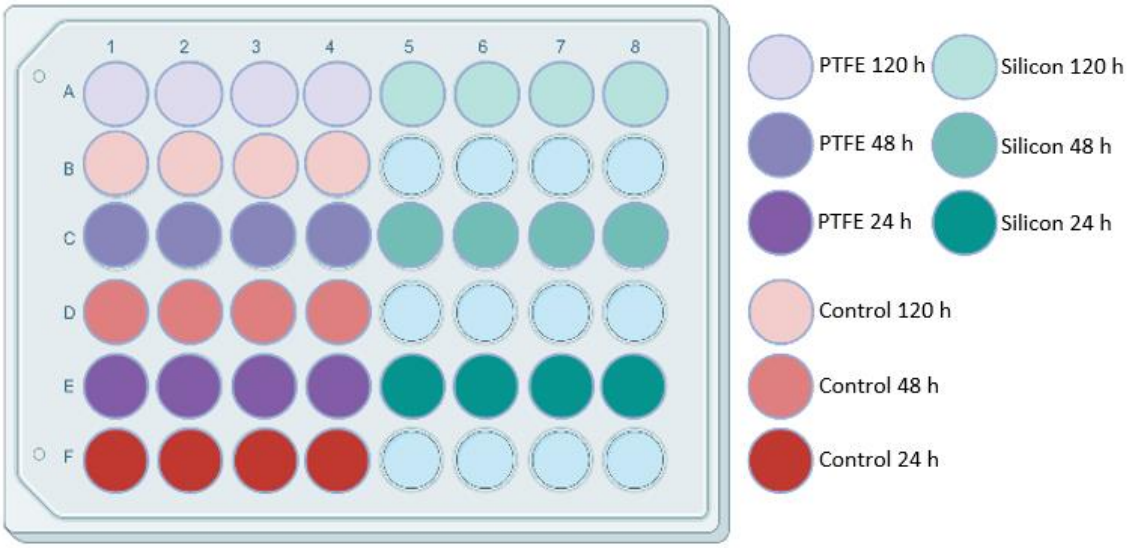

Figure 7: Pipetting scheme for testing the material of the cultivation chambers. The times given in the legend refer to the different incubation times of the conditioned and control media used (created with BioRender).

The adherent adMSC in 2D monolayer culture were exposed to the conditioned and control cell culture media for 48 h until the metabolic activity of the cells was measured fluorometrically by performing the resazurin-based Tox-8 assay according to 2.9.1. 200 µL Tox-8 working solution was pipetted into each of the 36 wells of the 48-well plate. Moreover, the cells were stained with calcein AM and propidium iodide to assess cellular viability or cell death, respectively. The staining was performed according to 2.9.2, whereby 120 µL staining solution containing both dyes in the stated concentrations was pipetted into each of the 36 wells of the 48-well plate.

2.1.2 Evaluation of the evaporation during cultivation in the Oli-UP system

As there were no data on gas exchange during the 3D expansion of cells in the Oli-UP cell culture system available, the evaporation of medium from the cultivation chambers during the cultivation was assessed. The evaporation rate is an important parameter as a high value could alter the osmolarity which could in turn affect cell growth. To assess the evaporation rate, five silicon and five PTFE cultivation chambers were filled with 1 mL cell culture medium each. The chambers placed in the autoclavable boxes were incubated for 24 hours at 37°C and 5 % CO_2 under ambient oxygen conditions. After 24 hours, the remaining volume of the medium was measured by taking it up with a 1000 µL pipette. The intake volume on the pipette was thereby adjusted until the remaining amount of medium in the chambers could be determined.

2.2 Characterization of cell growth of primary adMSC

Before cultivating the adMSC in the Oli-UP 3D cell culture system, the cell growth of primary adMSC was characterized under normoxic (21 % oxygen) and hypoxic (5 % oxygen) conditions by using a novel cell microscope provided by the company PHIO scientific GmbH. This microscope equipped with a camera offered the possibility to automatically record data on cell proliferation by tracking the cell-covered area (confluency) over time. A data point is recorded every 30 minutes. The cellwatcher microscope is connected to a control display and a minicomputer that was further connected to a local area network for real-time tracking.

2.2.1 Cells and medium used for the characterization of cell growth

To characterize the cell growth behavior of primary mesenchymal stem cells, adMSC 101220 in passage 0 were used. The cells were stored in the liquid nitrogen tank, thawed, and directly seeded on a T-75 flask for monitoring the growth behavior. For the expansion at 21 % O_2, the cells were cultured at 37°C and 5 % CO_2 under normal oxygen conditions, whereas the cells have also been isolated under these conditions. For monitoring the growth behavior under hypoxic conditions, the cells were cultured at 37°C, 5 % CO_2, and 5 % O_2, whereby those cells have also been isolated at 5 % O_2.

For the cultivation of the primary adMSC cell culture medium was used.

2.2.2 Experimental design

For the cultivation under both oxygen concentrations, the cells were thawed on day 0 and seeded on a T-75 flask, and incubated overnight under the respective conditions. On day 1, the medium was changed whereby 15 mL of fresh cell culture medium were added to the flasks. Directly after the media change, the flasks were placed in the cell microscope and recording was started. The cells were cultured and passaged two times at a confluency of around 75 %. For both conditions tested, the seeding density after the first passage was 4000 cells/cm^2 and 2500 cells/cm^2 after the second passaging procedure. After seeding the cells into the T-75 flasks, the respective flasks were swirled several times in a uniform horizontal figure-eight movement to achieve a homogeneous distribution of the cells. After that, the flasks were put back in the cellwatcher microscope for further analysis, whereby the

measurement was continued after an adhesion phase of 30 minutes. The characterization of the cell growth of the primary adMSC under the different oxygen conditions was ended three days after the second passaging procedure. The different conditions were observed consecutively as only one microscope was available. Figure 8 below shows the composition of the cellwatcher microscope.

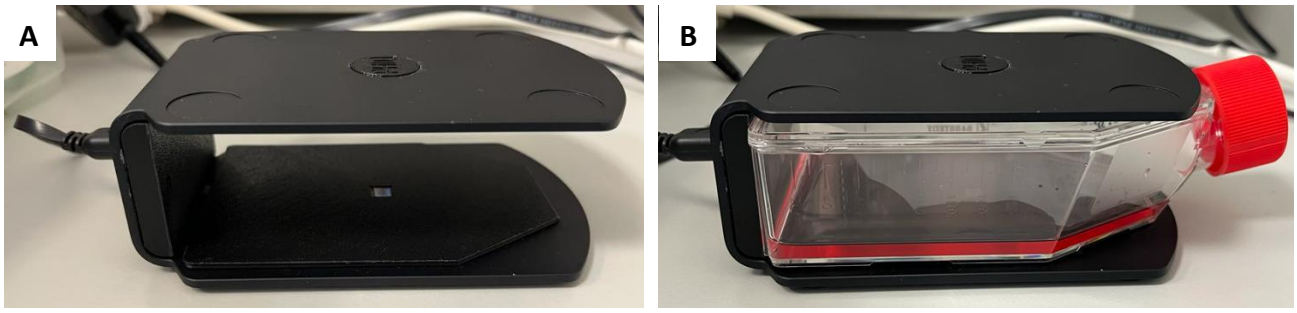

Figure 8: PHIO cellwatcher microscope for characterization of cell growth (A-B). A) frame of the microscope with the camera in the middle of the bottom side of the microscope, B) T-75 flask inserted for recording data.

Cell proliferation and growth behavior were analysed by evaluation of the area covered by cells (confluency) over time for both oxygen concentrations followed by the calculation of the dedicated population doubling times.

2.3 Cultivation in Oli-UP 3D cell culture system

For the expansion of adMSC in a physiologic 3D environment, the cells were embedded in hydrogel and cultured in the Oli-UP 3D cell culture system in a vertical way. The growth behavior of primary adMSC was compared to that of the immortalized cell line adMSC K5 under normoxic and hypoxic oxygen conditions, resulting in four different conditions being observed.

2.3.1 Hydrogel, cells, and medium used for the 3D cultivation in the Oli-UP

For the 3D cultivation of the MSC in the Oli-UP cell culture system, the photocrosslinkable extracellular matrix gel LunaGel™ was used. The hydrogel has a stiffness of 0-6.5 kPa that can individually be adjusted via the photocrosslinking technology by controlling the duration of light exposure. For the cultivation in the Oli-UP cell culture system, a crosslinking time of two minutes was chosen. With this light exposure time a compromise between, the stiffness of the gel, the cell viability and the cell spreading ability could be found.

For the experiment, the primary cells adMSC 101220 in passage 0 and the cell line adMSC K5 in passage 7 were used. Both stem cell types were stored in the liquid nitrogen storage tank, thawed, and seeded on T-75 flasks. Both cell types were expanded at 37°C, 5 % CO_2, and 21 % O_2 for two passages in cell culture flasks until they were embedded into the hydrogel for 3D cultivation. For the first experiment, the cells were only cultured under normal oxygen conditions at 37°C and 5 % CO_2.

For the 2D expansion on T-flasks as well as for the 3D cultivation in hydrogel, cell culture medium was used for both stem cell types.

2.3.2 Experimental design

The Oli-UP 3D cell cultivation system consists of various components that are all reusable and autoclavable and need to be assembled for 3D cultivation. The scaffold holders made of silicon were placed on the supporting elements and put down on the seeding plates in one of the autoclavable boxes horizontally. Before starting the cultivation in the Oli-UP, the assembled system was packed into sterilization foil and was autoclaved. For pouring the hydrogels, the Lunagel™ solution was prewarmed in the water bath at 37°C to become liquid, whereas the lyophilized photoinitiator was reconstituted in PBS. The cells were detached, counted and the required volume of cell suspension was transferred to a 15 mL tube. The cells were always encapsulated in the Lunagel™ at a concentration of $0.5 \cdot 10^6$ cells/mL hydrogel. The cell suspension was centrifuged, and the pellet was resuspended in equal volumes of Lunagel™ solution and photoinitiator solution by carefully pipetting up and down. 95 µL hydrogel containing the encapsulated cells were then transferred into the small ports of the scaffold holders. The scaffold holders placed on the supporting elements were transferred into the Luna Crosslinker™, covered with the lid of a well plate of choice and the gel was crosslinked for two minutes through UV light exposure. After successful crosslinking, the supporting elements still connected to the scaffold holders were transferred back into the autoclavable boxes and incubated for one hour at 37°C, 5 % CO_2, and 21 % O_2 for the hydrogels to become more compact. The scaffold holders containing the cell-laden constructs were then removed from the supporting elements and transferred in a vertical position into the 5-well cultivation chambers placed in another type of autoclavable box and filled with 1 mL cell culture medium. For the experiment, the cultivation chambers made of silicone were

used as their cleaning and handling were easier. Before use, those boxes containing the chambers were also packed into sterilization foil and autoclaved. The whole boxes were then incubated at 37°C, 5 % CO_2, and 21 % O_2 on a shaker at 100 rpm for 3D expansion of the different stem cell types. As controls, hydrogels without cells (blanks) were casted using the same procedure and were treated the same as those containing cells. The components of the Oli-UP 3D cell culture system are depicted in Figure 9.

Components of the Oli-UP 3D cell culture system

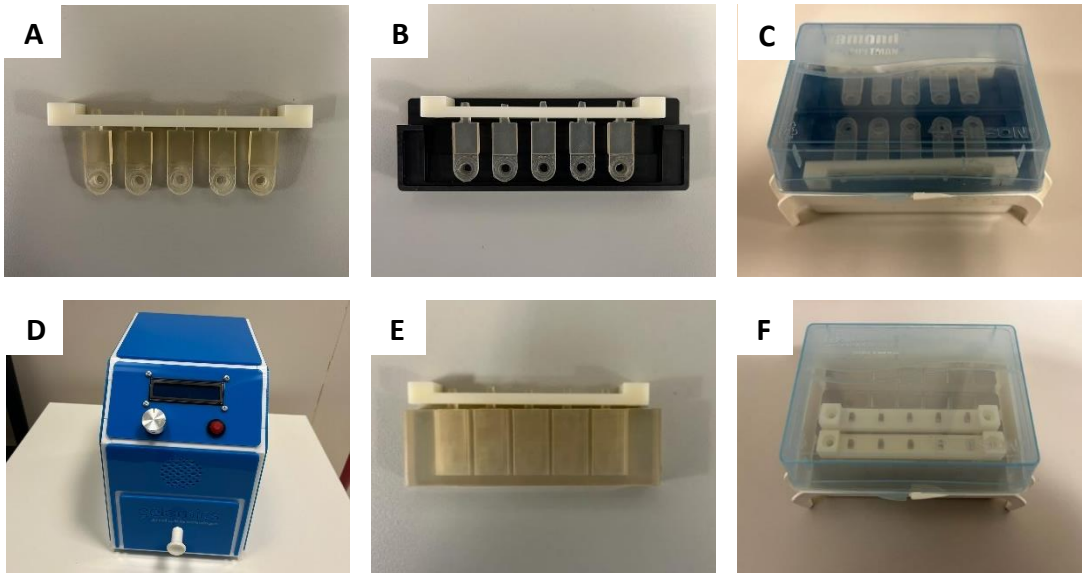

Figure 9: Components of the Oli-UP system for 3D cultivation of cells (A-F). A) scaffold holder made of silicon, B) scaffold holder placed on supporting element, C) placed in the autoclavable box on the seeding plate for pouring the hydrogels, D) crosslinking of hydrogels in Luna Crosslinker™, E) transfer to 5-well cultivation chambers filled with cell culture medium, F) 3D vertical cultivation in autoclavable box.

On day 0, day 4, and day 7 of cultivation, the metabolic activity of the cells was measured fluorometrically by performing the Tox-8 assay according to 2.9.1. On each analysis day, three control gels (blank control) and five hydrogels containing cells were transferred from the scaffold holders to a 96-well plate with a spatula and covered with 120 µL Tox-8 working solution per hydrogel. On the respective days, the hydrogels were additionally stained with calcein AM and propidium iodide to visualize live and dead cells. The staining was performed according to 2.9.2, whereby on each analysis day two hydrogels containing cells were transferred to a 96-well plate and covered with 100 µL staining solution containing both dyes in the stated concentrations. For day 0 analytics, the hydrogels were directly transferred to the 96-well plates after the incubation period of one hour. On day 4, the medium was removed, and 1 mL fresh cell culture medium was added per cultivation chamber.

2.4 Evaluation of the crosslinking procedure

As the results concerning the 3D cultivation of the different stem cell types in the Oli-UP cell culture system in 3.3 were not as expected, it was evaluated if the crosslinking procedure of the hydrogel in the silicon scaffold holders affects cell growth. The wavelength of the light in the Luna Crosslinker™ could interfere with the material of the scaffold holders and leach some toxic components that could further impact cellular behavior.

2.4.1 Hydrogel, cells, and medium used for evaluating the crosslinking procedure

For the evaluation of the crosslinking procedure adMSC K5 cells in passage 14 were embedded in the photocrosslinkable LunaGel™. The cells were stored in the liquid nitrogen storage tank, thawed in passage 7, and cultured in T-flasks at 37°C, 5 % CO_2, and 21 % O_2. The cells were passaged seven times until they were embedded into the hydrogel for 3D expansion.

For the 2D and 3D cultivation of the immortalized cell line adMSC K5, cell culture medium was used.

2.4.2 Experimental design

To rule out that the crosslinking procedure affects cell growth, three different cultivation conditions were tested. For the experiment, the Oli-UP 3D cell culture system was assembled and prepared as described in section 2.3.2, except the autoclavable boxes containing the 5-well cultivation chambers were not needed. In two of the three conditions examined, the cells were mixed with hydrogel and photoinitiator and were poured into the small ports of the scaffold holders placed on the supporting elements as described in 2.3.2. As delineated in this section, the hydrogels were crosslinked inside the scaffold holders in the Luna Crosslinker™ for two minutes and were incubated for one hour at 37°C, 5 % CO_2, and 21 % O_2 afterward. For the first cultivation condition, the scaffold holders containing the cell-laden constructs were transferred into a petri dish with a diameter of 150 mm filled with 10 mL cell culture medium. For the second condition, the hydrogels were removed from the scaffold holders with a spatula and transferred into a 96-well plate for cultivation in 130 µL cell culture medium. For testing the third cultivation condition, the cells were detached and mixed with

equal volumes of Lunagel™ solution and photoinitiator solution as described in section 2.3.2. For crosslinking, 95 µL of the hydrogel containing the encapsulated cells was pipetted into the wells of the 96-well plate. To prevent cell adhesion on the well bottoms, the wells were coated with agarose before. The whole plate was transferred into the Luna Crosslinker™ and the hydrogels were exposed to the UV light for two minutes. After the crosslinking procedure, the gels were covered with 130 µL cell culture medium and were directly cultivated in the 96-well plate. Five hydrogels were poured per condition, whereby the cells were encapsulated in the Lunagel™ at a concentration of $0.5 \cdot 10^6$ cells/mL hydrogel in all three terms. The cells were cultured at 37°C, 5 % CO_2, and 21 % O_2 for four days.

On day 4 of cultivation, the metabolic activity of the cells was measured fluorometrically by performing the Tox-8 assay according to 2.9.1. Three hydrogels per condition were transferred to a 96-well plate with a spatula and covered with 120 µL Tox-8 working solution. As a reference, the metabolic activity of three samples prepared for the second cultivation condition was also measured on day 0 after successful crosslinking. To assess cellular viability or cell death the hydrogels were additionally stained with calcein AM and propidium iodide. The staining was performed according to 2.9.2 whereby two hydrogels of each condition were transferred to a 96-well plate and covered with 100 µL staining solution containing both dyes in the stated concentrations.

2.5 3D cultivation in PEEK cultivation chambers

The company LifeTaq Analytics provided new cultivation chambers made of the chemically inert material polyetheretherketone (PEEK) for the 3D cultivation of adMSC in the Oli-UP cell culture system. Although it could be shown in section 3.1.1 that the non-medical grade materials silicone and PTFE of the cultivation chambers do obviously not affect cell growth, it could not entirely be excluded that the cell behavior is not a bit impacted. With the 5-well PEEK chambers, it can be ensured that the material does not interfere with cell growth.

2.5.1 Hydrogel, cells, and medium used for the 3D cultivation in PEEK chambers

For the 3D expansion in the PEEK cultivation chambers of the Oli-UP cell culture system, the photocrosslinkable GelMA-based hydrogel called LunaGel™ was utilized.

For the experiment, the cell line adMSC K5 in passage 13 was chosen. The cells were stored in the liquid nitrogen storage tank, thawed in passage 7, and cultured in T-flasks at 37°C, 5 % CO_2, and 21 % O_2. The cells were passaged six times until they were embedded into the hydrogel for 3D cultivation.

For the 2D expansion of the cell line on T-flasks as well as for the 3D cultivation of the cells embedded in hydrogel, cell culture medium was used.

2.5.2 Experimental design

For the 3D cultivation of the cell line in the Oli-UP cell culture system, the procedure was conducted as described in section 2.3.2, with the PEEK cultivation chambers being used instead of the silicone chambers. Six hydrogels were poured with the adMSC K5 being encapsulated in the Lunagel™ at a concentration of $0.5 \cdot 10^6$ cells/mL hydrogel. Control gels without cells have not been casted in that experiment. The cells were cultured at 37°C, 5 % CO_2, and 21 % O_2 over a period of seven days.

Analysis was performed on day 0, day 4, and day 7 by staining the cells with calcein AM and propidium iodide according to 2.9.2 to assess cellular viability and cell death. On each analysis day, two hydrogels were transferred to a 96-well plate and covered with 100 µL staining solution containing both dyes in the stated concentrations. For day 0 analytics, the hydrogels were directly transferred to the 96-well plate after the incubation period of one hour. The medium was changed on day 4 by adding 1 mL of fresh cell culture medium per cultivation chamber.

2.6 6-well plate cultivation

As the technical problems with the 3D cultivation in the Oli-UP cell culture system could not be solved together with the manufacturer LifeTaq Analytics, an alternative setup was compiled. Instead of cultivating the cells embedded in hydrogels in a vertical way in the Oli-UP cultivation chambers, they were expanded horizontally in 6-well plates. Primary adMSC and the immortalized cell line adMSC K5 were grown under normoxic and hypoxic oxygen conditions to validate the growth behavior of both cell types under the different conditions being observed.

2.6.1 Hydrogel, cells, and medium used for the 6-well plate cultivation

For the 3D expansion of both stem cell types in the 6-well plate setup, the photocrosslinkable GelMA-based LunaGel™ was used.

To validate the cell proliferation of the different stem cell types, the cells were expanded in 2D on T-flasks at 37°C, 5 % CO_2, and 21 % O_2 and only incubated under the different oxygen concentrations during 3D cultivation. For the experiment, the primary cells adMSC 101220 in passage 0 isolated under normoxic oxygen conditions and stored in the liquid nitrogen tank were thawed and seeded on T-75 flasks. The cells were expanded for one passage in cell culture flasks in a humidified incubator under normal oxygen conditions at 37°C, 5 % CO_2 until they were embedded in the photocrosslinkable LunaGel™ for 3D cultivation at 21 % O_2 and 5 % O_2, respectively. The cell line adMSC K5 in passage 7 was stored in the liquid nitrogen storage tank, thawed, and seeded on a T-75 flask. The cells were expanded for three passages in cell culture flasks until they were embedded in the hydrogel for cultivation at 21 % O_2. For the 3D cultivation under hypoxic conditions, the cells were passaged another three times while being cultured at 37°C, 5 % CO_2, and 21 % O_2 until the cells in passage 13 were finally embedded in the hydrogel for cultivation at 5 % O_2. Table 1 below provides an overview of the stem cell types used in the experiment.

Table 1: Overview of the cells used during 6-well plate cultivation under different oxygen concentrations

Primary adMSC		**Cell line adMSC K5**	
Normoxia (21 % O_2)	Hypoxia (5 % O_2)	Normoxia (21 % O_2)	Hypoxia (5 % O_2)
adMSC 101220 NORM in p1	adMSC 101220 NORM in p1	adMSC K5 NORM in p13	adMSC K5 NORM in p10

For the 2D and 3D cultivation of both stem cell types, cell culture medium was used.

2.6.2 Experimental design

In principle, the experimental procedure was conducted as described in section 2.3.2. However, instead of transferring the scaffold holders containing the cell-laden hydrogels from the supporting elements into the 5-well cultivation chambers, one single scaffold folder was placed in each well of a 6-well plate for cultivation. Each well was filled with 4 mL cell culture medium. The 6-well plates were then incubated at 37°C, 5 % CO_2, and the respective oxygen conditions on a shaker at 100 rpm for 3D expansion of the different stem cell types. As controls, hydrogels without cells (blanks) were casted using the same procedure and were treated the same as those containing cells. The basic workflow for the 3D expansion of the cells in the 6-well plates is depicted in Figure 10.

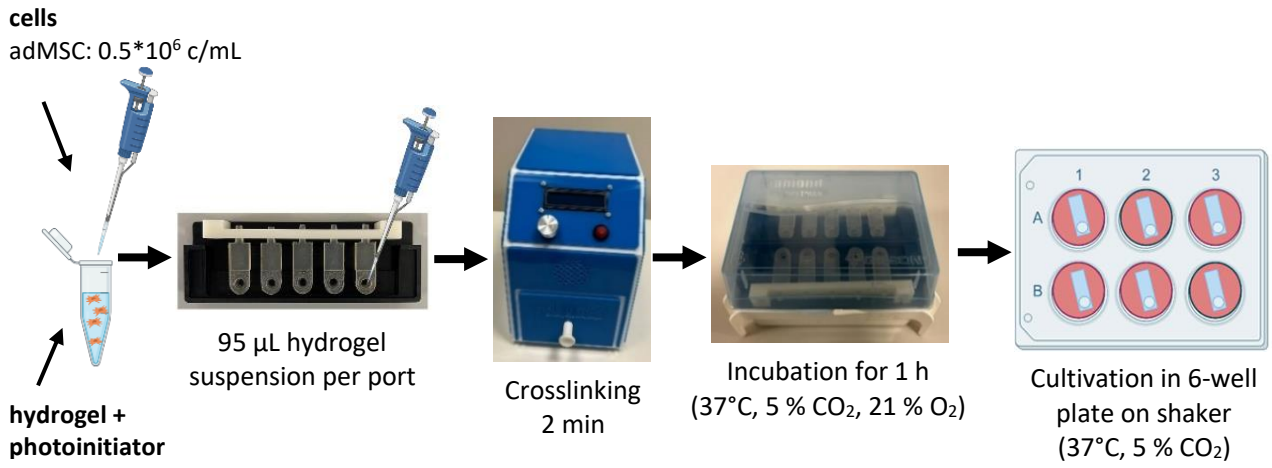

Figure 10: Schematic overview of the basic workflow for 3D cultivation of adMSC in 6-well plates (created with BioRender).

Cell growth was validated on day 0, day 4, and day 7 of cultivation by measuring the metabolic activity and by assessing the cellular viability and cell death with the live/dead staining as delineated in section 2.3.2. On day 4, the medium was removed, and 4 mL fresh cell culture medium was added per well.

2.7 Hydrogel expansion

Despite the technical problems with the 3D expansion of adMSC in the Oli-UP 3D cell culture system could not be solved, the future perspective is to fully automate the cultivation of cells in this system. For this continuous 3D expansion of cells, a preliminary trial was conducted to evaluate the feasibility of passaging cells while being embedded in a hydrogel.

2.7.1 Hydrogel, cells, and medium used for the hydrogel expansion

For the experiment, adMSC K5 cells in passage 8 were embedded in the photocrosslinkable LunaGel™. The cells were stored in the liquid nitrogen storage tank, thawed in passage 7, and seeded on a T-75 flask. The cells were expanded at 37°C, 5 % CO_2, and 21 % O_2 for one passage until they were embedded into the hydrogel for 3D cultivation.

For the 2D expansion of the cell line on T-flasks as well as for the 3D cultivation of the cells embedded in hydrogel, cell culture medium was used.

2.7.2 Experimental design

Although the Oli-UP cell culture system was not applied for the cell expansion in this experiment, the scaffold holders were utilized for molding the hydrogels. For the hydrogel expansion, the Oli-UP 3D cell culture system was assembled and prepared as described in section 2.3.2, apart from the autoclavable boxes containing the 5-well cultivation chambers, which were not needed in this setup. The cells were detached, mixed with equal volumes of hydrogel solution and photoinitiator solution, and were then poured into the small ports of the scaffold holders placed on the supporting elements as delineated in this section. The hydrogels were crosslinked inside the scaffold holders in the Luna Crosslinker™ for two minutes and were incubated for one hour at 37°C, 5 % CO_2, and 21 % O_2 afterward for the gels to become more compact. As controls, hydrogels without cells (blanks) were casted using the

same procedure and were treated the same as those containing cells. After the incubation period of one hour, the hydrogels were transferred with a spatula to a 96-well plate for cultivation in 130 µL cell culture medium at 37°C, 5 % CO_2, and 21 % O_2.

The cells embedded in LunaGel™ were passaged on day 4 and day 9. Therefore, five cell-laden hydrogels were put into a 15 mL tube and were homogenized with a mortar suited for this tube size. Three hydrogels without cells were homogenized in another tube serving as blank controls. Fresh LunaGel™ mixed with photoinitiator was then added at a ratio of 1:3.5 to both tubes containing the homogenized hydrogels. After carefully mixing by pipetting up and down using a pipette with a cut tip, fresh hydrogels were poured into the molds of the scaffold holders of the Oli-UP and crosslinked according to the procedure described in section 2.3.2. After passaging the adMSC K5 twice, the cells were further cultivated for another few days. An overview of the workflow for the hydrogel expansion is illustrated in Figure 11 below.

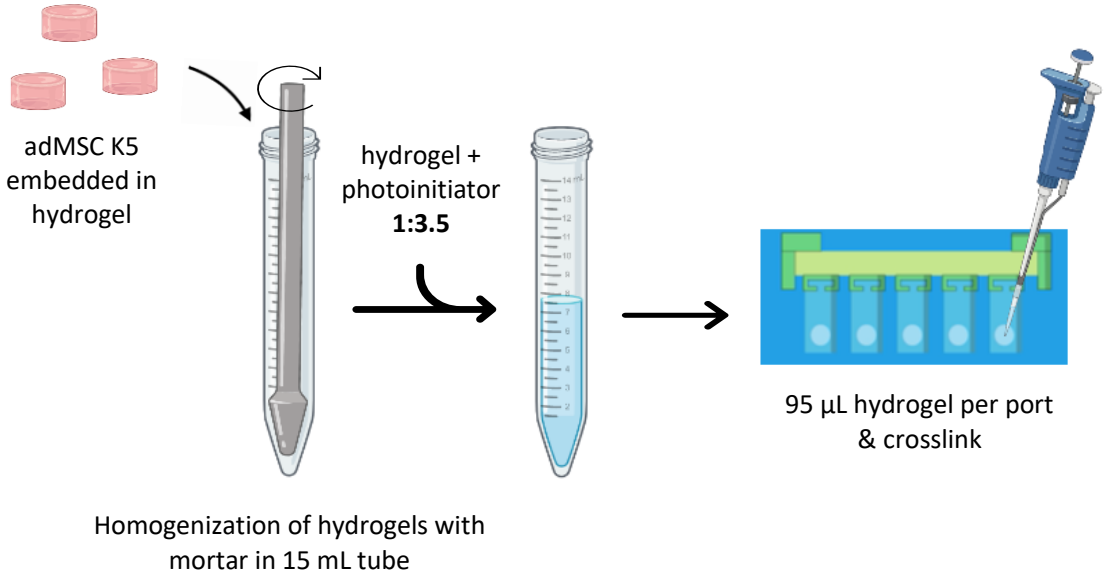

Figure 11: Schematic overview of workflow for 3D hydrogel expansion (created with BioRender).

For the evaluation of the hydrogel passaging approach, the metabolic activity of the cells was measured on day 0 as well as on day 4 and day 7 before and after the passaging procedure by performing the resazurin-based Tox-8 assay according to 2.9.1. On each analysis day, three control gels (blank control) and three hydrogels containing cells were transferred to a fresh 96-well plate with a spatula and covered with 120 µL Tox-8 working solution per hydrogel. On the respective days as well as on day 14 and day 21 of the cultivation, the hydrogels were additionally stained with calcein AM and propidium iodide to visualize live and dead cells. The

staining was performed according to 2.9.2 whereby two hydrogels containing cells were transferred to a 96-well plate and covered with 100 µL staining solution containing both dyes in the stated concentrations. For day 0 analytics, the hydrogels were directly transferred to the 96-well plates after the incubation period of one hour.

2.8 Statistical analysis

The Tox-8 data of the different experiments are presented as mean ± the standard deviation (SD) with at least three independent replicates. The respective sample size "n" of the experiment is given in the legend of each corresponding figure. Normal distribution of the data was checked prior to the analysis using suitable normality tests. The significance is indicated in the plots as follows: * $p < 0.05$, ** $p < 0.01$, *** $p < 0.001$, **** $p < 0.0001$. All statistical analysis were carried out using GraphPad Prism 9.

2.9 Analytical methods

2.9.1 Tox-8 assay

To measure the metabolic activity of living cells, the In Vitro Toxicology Assay Kit (TOX8-1KT) was used. This assay is based on the oxidoreduction indicator dye resazurin. Viable cells reduce the oxidized form of the dye, which is dark blue, to the red fluorescent resorufin form. The amount of the conversion can then be measured fluorometrically or spectrophotometrically. In the scope of this thesis, the resazurin solution was added to the cells in an amount equal to 10 % of the culture medium volume. Analysis was always performed in multiwell plates. After adding the Tox-8 working solution, the plates were incubated on a horizontal shaker at 100 rpm for three hours at 37°C and 5 % CO_2. After the incubation period, 100 µL supernatant was transferred into fresh wells of a 96-well plate. Fluorescence intensity was then measured using a Tecan plate reader at an emission wavelength of 590 nm and an excitation wavelength of 560 nm. A gain of 100 was used for all measurements.

2.9.2 Calcein AM propidium iodide staining

To assess cellular viability or cell death as well as for morphological examination, cells were stained with calcein acetoxymethyl ester (calcein AM) and propidium iodide. The cell-permanent dye calcein AM is used to assess cell viability as it can easily enter intact cells. The staining is based on the fact that living cells enzymatically convert the nonfluorescent calcein AM to the green-fluorescent calcein in their cytoplasm. During the enzymatic conversion calcein AM is hydrolyzed by intracellular esterases. Compared to that the fluorescent dye propidium iodide can only enter dead cells with non-intact membranes and is therefore used to identify dead cells. When entering dead cells, the intercalating dye propidium iodide binds nucleic acids in a linear way. Once the dye is bound the fluorescence signal increases, whereby the fluorescently labeled dead cells appear red. In the scope of this thesis, both dyes were used together to assess cell viability and cell death. For the staining, the adherent cells or cell-laden hydrogels were incubated at a final concentration of 1 µg/mL calcein AM and 3.3 µg/mL propidium iodide in cell culture medium for 30 minutes at 37°C and 5 % CO_2 in the dark on a horizontal shaker. After the incubation period, the samples were rinsed three times with prewarmed PBS, covered with PBS, and analyzed with a fluorescent microscope, equipped with a camera.

3 Results and Discussion

3.1 Characterization of the Oli-UP 3D cell culture system

3.1.1 Testing the materials of the cultivation chambers

For screening the materials of the Oli-UP cultivation chambers for toxic leachables, adherent adMSC were exposed to conditioned cell culture media for 48 h followed by measuring the metabolic activity and by staining the cells with calcein AM and propidium iodide. As a control, cells were cultured in standard cell culture medium.

The results of the Tox-8 assay show that there is no distinct difference in metabolic activity between the control and the cells exposed to the different conditioned media containing the potentially toxic components (see Figure 12). This observation applies particularly to the media conditioning periods of 48 h and 120 h. However, for the media conditioned for 24 h, the signal detected for the control was slightly lower compared to the materials tested. Moreover, there is a slight decrease in metabolic activity with the extended incubation time of the media for both, the control and the materials tested. Statistical analysis revealed a significant difference between the control and the cells cultured in the media conditioned for 24 h in the PTFE cultivation chambers as well as between the control and the cells exposed to the media conditioned for 24 h in the chambers made of silicone.

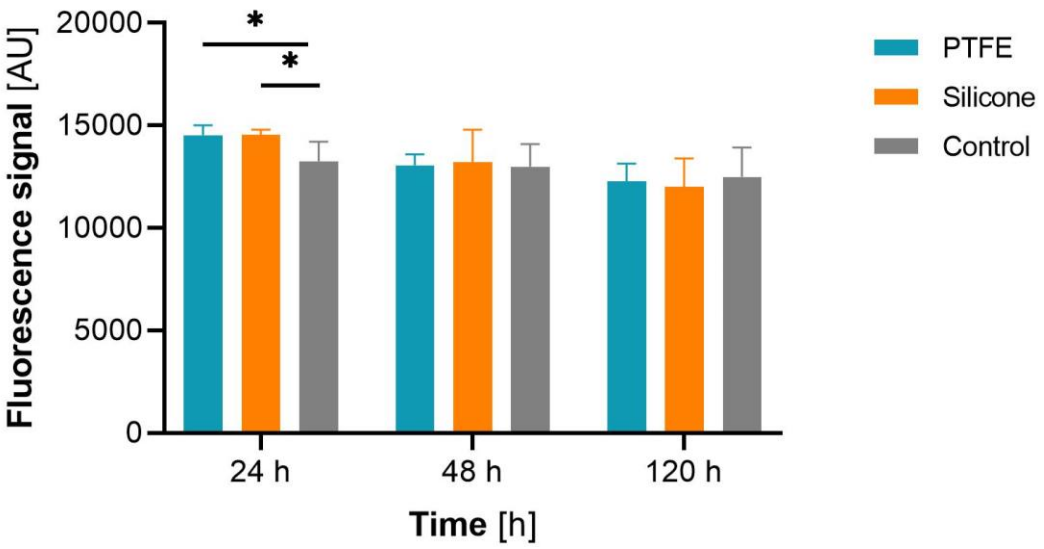

Figure 12: Toxicity screening of materials of Oli-UP cultivation chambers. Adherent adMSC in 2D monolayer culture were exposed to conditioned and control cell culture medium for 48 h. For the media conditioning periods of 48 h and 120 h, the measurement of the metabolic activity revealed similar values for the control and the cells exposed to the different conditioned media. However, for the media conditioned for 24 h, the signal detected for the control was slightly lower compared to the materials tested (n=4, one-way ANOVA, significance determined using Tukey's multiple comparisons test, α= 0.05).

The live/dead staining (see Figure 13) resulted in equal numbers of viable cells, stained by calcein AM, in all three conditions tested. In all groups, only a minor number of dead cells, appearing red in the propidium iodide staining, was observed. Overall, the cells were evenly distributed forming a 2D monolayer whereas they have already grown rather confluent throughout the cultivation period of 48 h. Most cells showed an elongated, spindle-shaped morphology while growing plastic adherent which is typical for adMSC. Some round-shaped cells on top of the monolayer are also visible which can probably be attributed to the high confluency observed. However, the cell layers exposed to the media conditioned for 120 h seem to partly detach from the plastic surface.

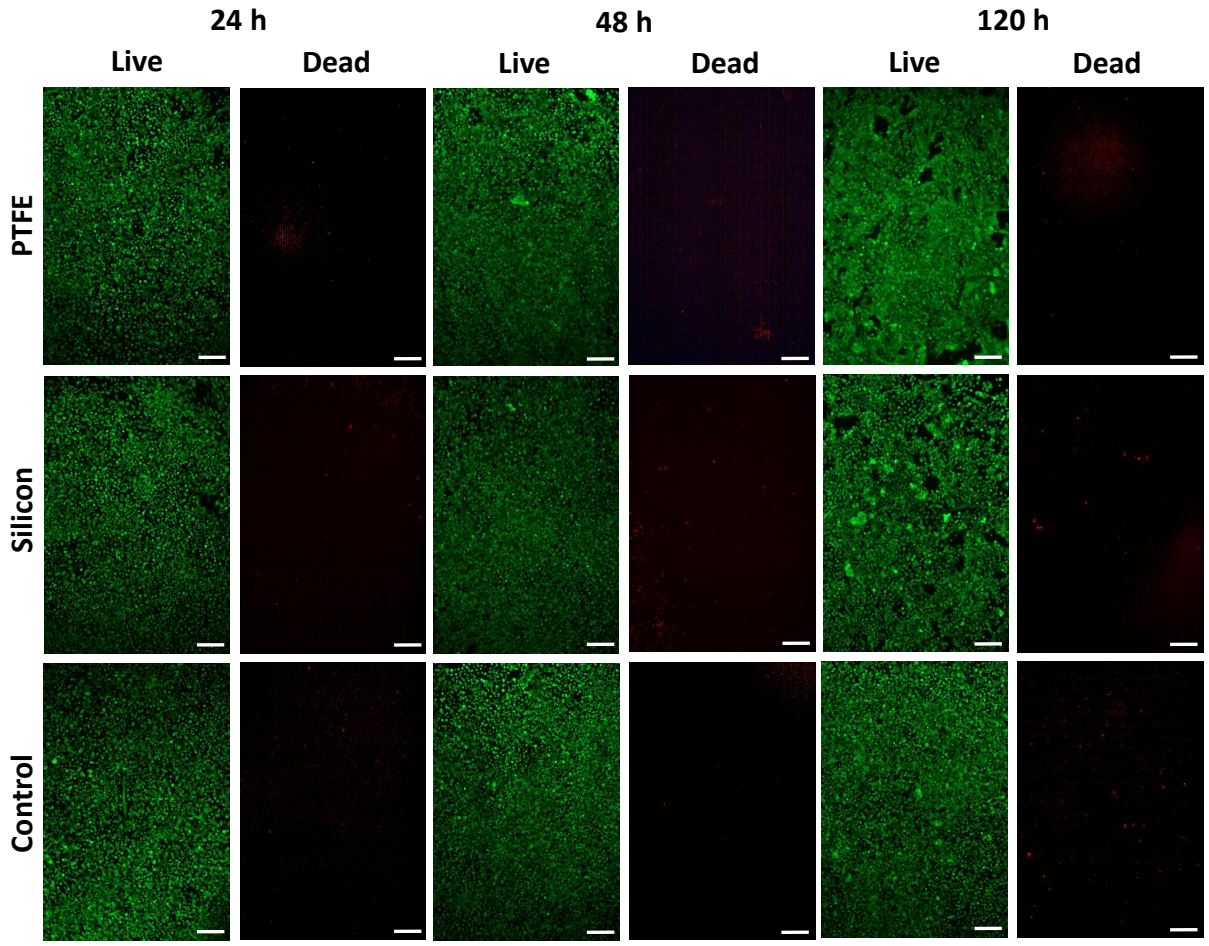

Figure 13: Live/dead staining of controls and cells exposed to conditioned media, green - calcein AM: viable cells, red - propidium iodide: dead cells. A high number of viable cells can be observed whilst only a minor number of dead cells is visible in all conditions tested. The cells are evenly distributed having already grown quite confluent over the course of cultivation (scale bar = 200 µm).

From those results, it could be concluded that the non-medical grade materials PTFE and silicone from which the Oli-UP cultivation chambers are made do not interfere with cell growth of the immortalized cell line adMSC K5. For the media conditioning period of 24 h, the metabolic assay revealed even a lower signal for the control compared to the tested materials. The decrease in metabolic activity with the extended incubation time could indicate that the composition of the cell culture medium changed over time during the incubation with fewer nutrients being available for cell proliferation. As the number of dead cells is rather small, the reason for the partly detaching cell layers overserved for the adMSC K5 exposed to the media conditioned for 120 h, might be that these cells were exposed to PBS the longest since these microscopy images were taken last. In that context, PBS is used to rinse and cover the cell layer after the staining. Nevertheless, the buffer can impair cellular behavior upon extended exposure. Taken together, it could be ruled out with

a high degree of probability that components that are toxic to the cells leach from the materials of the cultivation chambers during the 3D cell expansion.

3.1.2 Evaluation of the evaporation during cultivation in the Oli-UP system

To assess the evaporation rate of cell culture medium from the Oli-UP cultivation chambers during 3D cell expansion, five silicon and five PTFE chambers were filled with 1 mL cell culture medium each. After 24 hours of incubation, the remaining volume of medium was determined by taking it up with a pipette and adjusting the intake volume.

It was found that more than 80 µL of medium evaporated on average within 24 h from both chamber types. Such a high evaporation rate could alter the osmolarity which could in turn affect cell growth. To counteract that, two 0.2 µm filters were integrated into the lid of the autoclavable boxes of the Oli-UP system to ensure proper gas exchange during cultivation. The autoclavable boxes were additionally covered with parafilm for cultivation as there always remained a small cleft when closing the boxes. With those measures, the evaporation rate within 24 h was checked again with an average evaporation volume of 14 µL for the PTFE chambers and 9 µL for the silicon cultivation chambers, respectively. The remaining volumes of medium after 24 h of incubation before and after setting measures are presented in Table 2.

Table 2: Remaining volumes of medium in cultivation chambers after 24 h of incubation

	Remaining volume of medium in standard system [µL]		**Remaining volume of medium after integration of filters [µL]**	
	PTFE chambers	Silicon chambers	PTFE chambers	Silicon chambers
	900	910	985	1000
	910	920	980	990
	920	905	985	985
	950	925	990	1000
	910	920	992	980
Average remaining volume [µL]	**918**	**916**	**986**	**991**
Evaporation volume [µL]	**82**	**84**	**14**	**9**

By integrating the filters in the lid of the autoclavable boxes, the evaporation rate could be lowered considerably conferring a proper gas exchange to guarantee that the cells are well supplied during cultivation in the Oli-UP 3D cell culture system.

3.2 Characterization of cell growth of primary adMSC

For the evaluation of the cell growth of primary adMSC under normoxic (21 % oxygen) and hypoxic (5 % oxygen) oxygen conditions, cell proliferation was tracked using the PHIO cell microscope equipped with a camera. The adMSC of the same type cultured under both oxygen conditions were passaged two times at a confluency of around 75 %.

The graphs in Figure 14 show the confluency plotted vs. time for both oxygen conditions and all three passages observed. The orange graphs depict the cell proliferation under normoxic conditions whereas the blue graphs correspond to the growth behavior under hypoxic oxygen concentrations. In general, the graphs show similar trends for the respective passages under both oxygen conditions, with cell proliferation being observed under all terms. The graphs corresponding to passage 1 both rise abruptly at the beginning with an even more intense

leap under hypoxic conditions. Compared to that, the charts delineating the cell proliferation during passage 2 and 3 all show an initial lag phase.

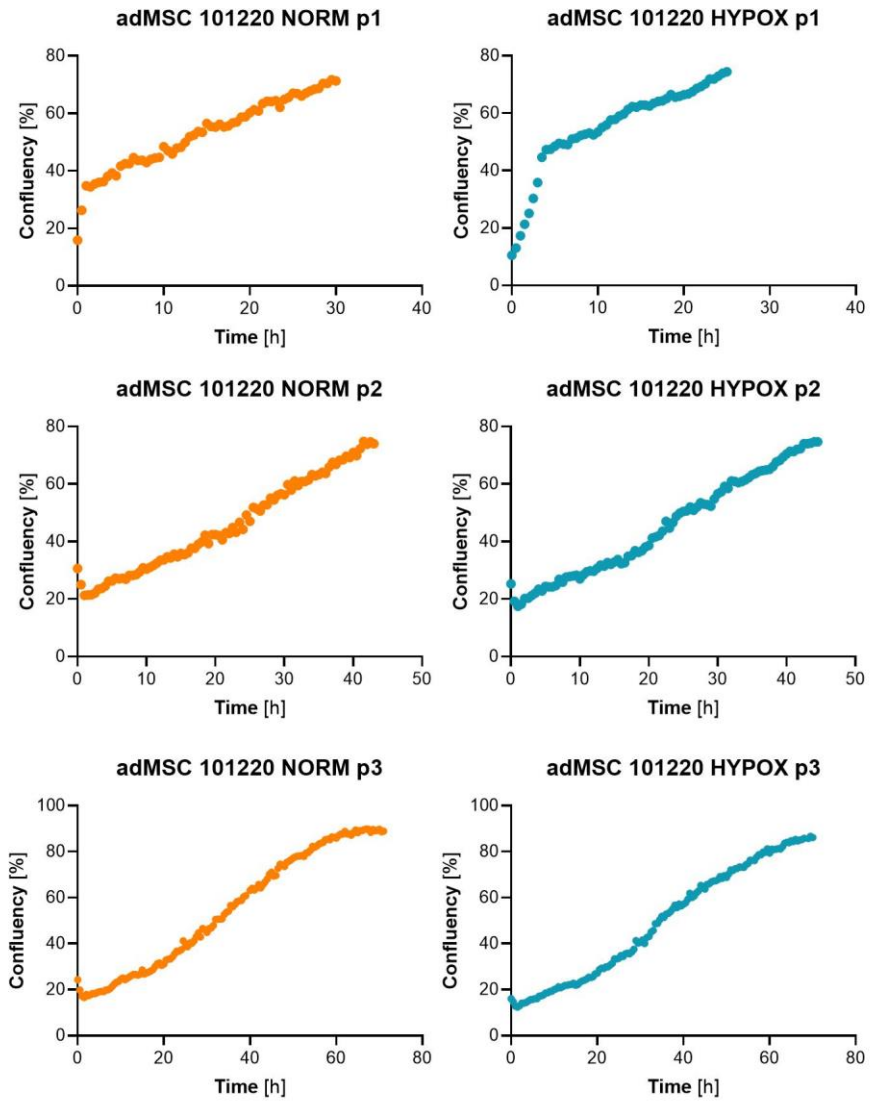

Figure 14: Cell proliferation of primary adMSC under normoxic and hypoxic oxygen conditions. The cell-covered area (confluency) was tracked overtime for three passages. The graphs show similar trends for the respective passages under the different oxygen conditions. The charts corresponding to passage 1 both rise abruptly at the beginning while the charts delineating the cell proliferation during passage 2 and 3 show an initial lag phase.

The abrupt rise of the graphs corresponding to passage 1 may result from the fact that the tracking was started on day 1 after thawing the cells right after changing media. And usually, the cryopreserved cells need some time to recover after thawing before they start proliferating. The initial lag phase observed for charts delineating the cell proliferation during passage 2 and 3 can be ascribed to the fact that the cells need some time to sediment after passaging, before becoming adherent again and proliferating further.

To finally compare the growth behavior of primary adMSC under the different oxygen conditions, the doubling times have been determined for each of the three passages for both oxygen concentrations using the confluencies tracked over time (see Figure 15).

For the calculation of the doubling times the following Equation 1 was used:

$$t_D = \frac{\ln\left(\frac{N(t)}{N_0}\right)}{\ln 2} \quad (1)$$

where t_D is the doubling time, $N(t)$ is the tracked confluency at time t and N_0 corresponds to the tracked confluency at time 0. Instead of the typically used cell numbers, the tracked confluencies were used for the calculation of the doubling times as only those parameters were traced by the cellwatcher microscope.

It can be observed that the doubling times are higher for the adMSC cultured under normoxic conditions (blue bars) in all three passages compared to the cells cultured under hypoxic conditions (orange bars). Moreover, the doubling times rise with each passage under both oxygen concentrations with an even more pronounced increase between the first two passages. Between these two passages, the doubling times have even tripled. The values presented have not undergone statistical analysis as only one value per time point was tracked by the microscope. This approach generally assumes that the cells observed are all the same size.

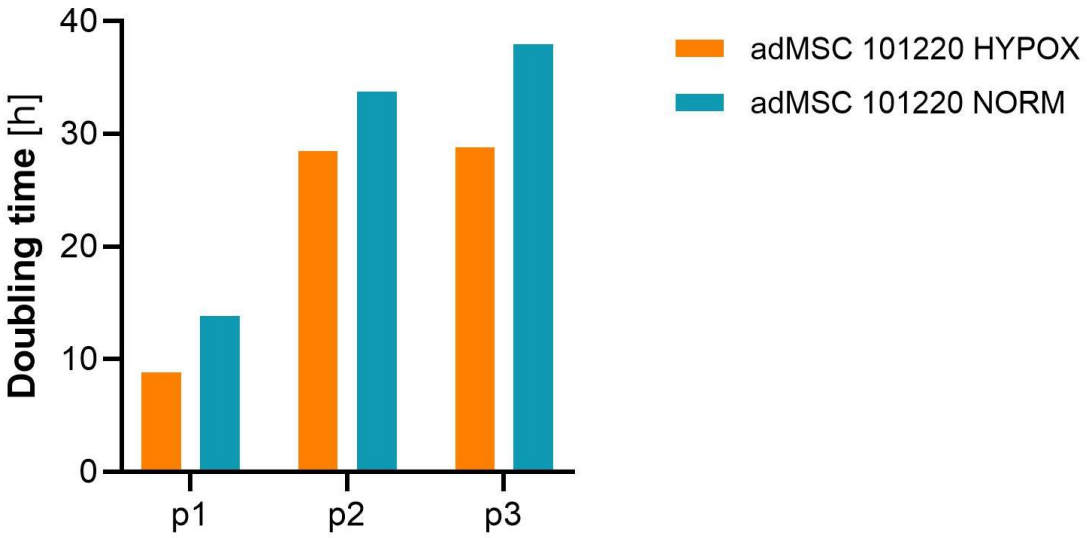

Figure 15: Doubling times established for each of the three passages for both oxygen conditions. The calculation of doubling times revealed higher values for the primary adMSC cultured under normoxia for all three passages. The doubling times generally rise with each passage over the course of cultivation under both oxygen concentrations.

The bar chart in Figure 16 shows the average doubling times over the cultivation period calculated for the cells grown under both oxygen conditions. Higher values can again be observed for the primary adMSC cultured at ambient oxygen conditions of 21 % represented

by the blue bar. While the average doubling time for the cells cultured under normoxia is slightly under 30 hours, the value revealed for the cells grown under hypoxia is marginally over 20 hours.

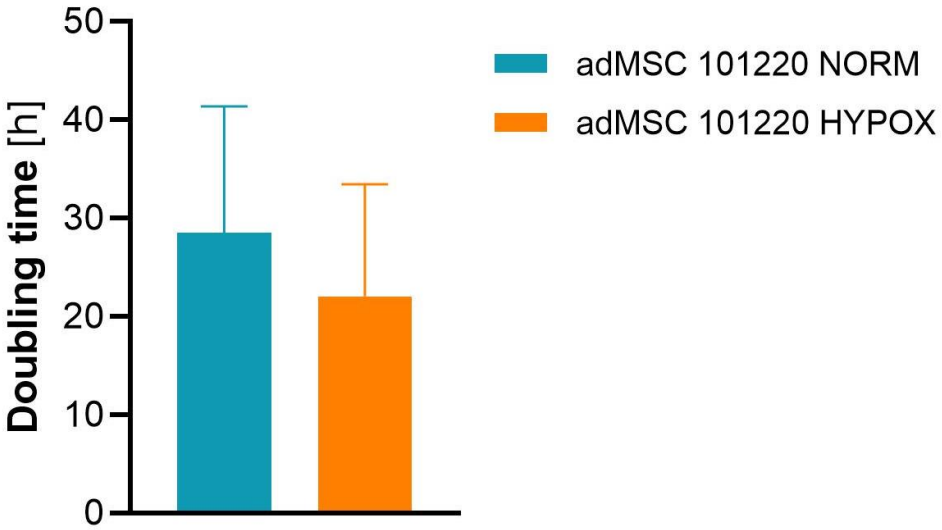

Figure 16: Average doubling times revealed for primary adMSC cultured at 21 % oxygen and 5 % oxygen, respectively. The average doubling time for the cells cultured at ambient oxygen conditions is around one quarter higher compared to the value obtained for cell growth under hypoxia.

The results of observing higher doubling times meaning slower cell growth under normoxic oxygen conditions were exactly what was expected as these findings are consistent with the results reported in literature [15][25]. The oxygen concentration is a crucial microenvironmental parameter for the physiologic cultivation of adMSC significantly affecting the cell behavior during cell expansion. As the average oxygen concentration in human tissues varies between 1 % and 15 % depending on the vascularization of the tissue, the ambient oxygen concentration of 21 % does not reflect the natural in vivo environment of adMSC. Consequently, increased cell proliferation is usually observed under hypoxic conditions.

The determination of the doubling times using the cell confluencies tracked over time assumes that all cells are of the same size, meaning that this calculation is likely to be subject to uncertainties. However, the actual purpose of the cell microscope is to trail cell proliferation in order to be able to estimate the time point when cells reach a certain confluency to be ready for passaging.

3.3 Cultivation in Oli-UP 3D cell culture system

For the 3D cell expansion in the gelatinemethylacyrol-based LunaGel™, primary adMSC as well as the immortalized cell line adMSC K5 were cultured in a vertical way in the Oli-UP 3D cell culture system. For comparison of the growth behavior of both cell types under normoxic and hypoxic oxygen conditions, the metabolic activity was determined followed by staining the cells with calcein AM and propidium iodide. As controls, hydrogels without cells (blanks) were casted and treated the same as those containing cells.

The Tox-8 data presented in Figure 17 are blank corrected and represent the cell metabolic activities measured on day 0, day 4, and day 7 under ambient oxygen conditions for both cell types. The primary adMSC as well as the immortalized cell line both show metabolic activity on day 0 after the cells were embedded in the hydrogel with the value for the primary adMSC being almost twice as high as that of the cell line. However, there is a significant decrease in signal over the course of cultivation for both cell types with nearly no metabolically active cells left on day 4 and day 7, respectively. Statistical analysis revealed a significant difference between the metabolic activities of both cell types measured on day 0, whereas the differences in the values obtained for day 4 and day 7 were not significant.

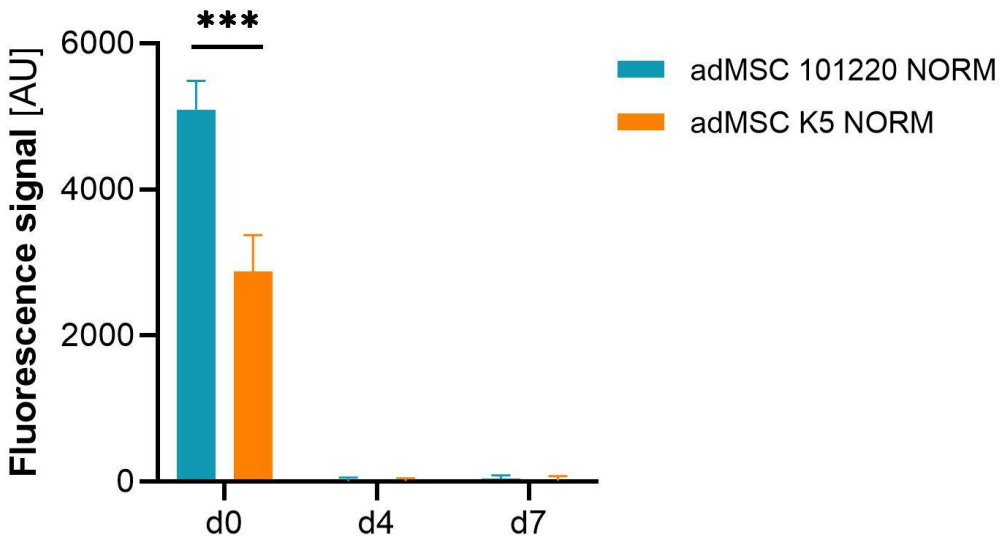

Figure 17: 3D expansion of primary adMSC and the immortalized cell line adMSC K5 in Oli-UP 3D cell culture system. The measurement of the metabolic activity revealed metabolically active cells on day 0 for both cell types with a significant decrease in signal throughout cultivation. On day 4 and day 7 hardly any fluorescence signals could be detected for both groups. The values presented are blanked (n=5, two-sided students t-test, α=0.05).

The live/dead staining (see Figure 18) showed up with similar results. On day 0 a high number of living cells, stained by calcein AM, was visible for both cell types with mostly round-shaped single cells being evenly distributed in the hydrogels. In both groups, only a small number of dead cells, stained by propidium iodide, were detected. However, only a few round-shaped living cells were visible on day 4 and day 7 with both stem cell types, whereas the bigger part of the cells appeared red in the propidium iodide staining meaning the cells died throughout the cultivation period of seven days.

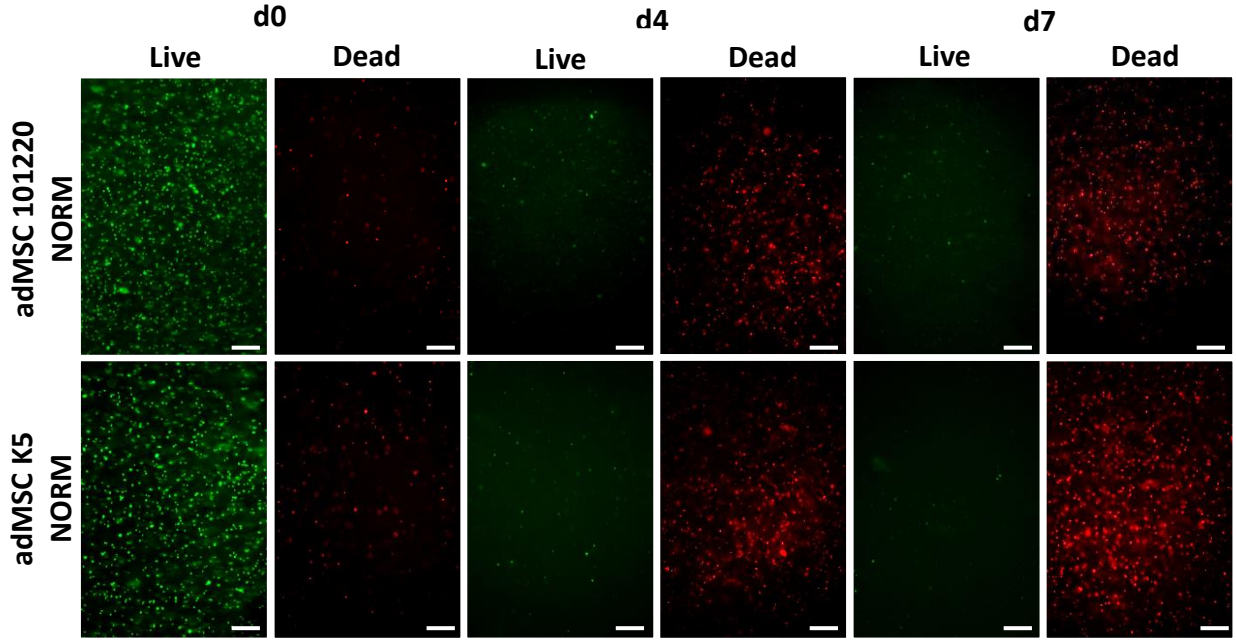

Figure 18: Live/dead staining of primary adMSC and adMSC K5 cultured at ambient oxygen conditions in Oli-UP 3D cell culture system, green - calcein AM: viable cells, red - propidium iodide: dead cells. A high number of evenly distributed viable cells can be observed on day 0 for both cell types whilst only a minor number of dead cells is visible. However, only a few living cells were detected on day 4 and day 7 for both stem cell types, whereas the bigger part of the cells died throughout the cultivation period of seven days (scale bar = 200 µm).

For the 3D expansion of the different stem cell types in the Oli-UP cell culture system, it would have been expected that the cells proliferate over the cultivation period of seven days. With rising cell numbers, the metabolic activities should have increased from day to day for both cell types what should have resulted in higher fluorescence signals detected in the Tox-8 assay. On day 0 the single cells appeared in a round shape as the images were taken directly after embedding the cells in the hydrogel. It usually takes the adMSC some time to become adherent, adapt their typical spindle-shaped morphology, and spread through the hydrogel that provides mechanical support. This is exactly what would have been expected to see in the calcein AM propidium iodide staining on day 4 and day 7. Instead, the minor number of living cells detected on day 4 and day 7 of the cultivation, still appeared in a round shape. The

cells should have spread in the hydrogels, which provide a convenient microenvironment for stem cell proliferation, and should have established cell-cell contacts forming a 3D network of cells. However, a large part of the initially seeded cells of both stem cell types died for an unknown reason during the 3D cultivation in the Oli-UP cell culture system. The figures only contain the metabolic activities as well as the live/dead staining observed under normoxic conditions as the 3D cell expansion was not successful, which is why the experiment was not conducted under hypoxic conditions for the time being.

3.4 Evaluation of the crosslinking procedure

To rule out that the hydrogel photocrosslinking procedure in the LunaCrosslinker™ impairs cell growth, adMSC K5 cells were cultured in three different settings to evaluate whether the wavelength of the light interferes with the silicon material of the scaffold holders leaching toxic components. After four days of cultivation, the metabolic activity was measured in all terms followed by staining the cells with calcein AM and propidium iodide. Condition 1 refers to the cells embedded in LunaGel™ followed by crosslinking in the scaffold holders and further cultivation in a petridish. In condition 2 the hydrogels containing the cells were photocrosslinked in the scaffold holders after being transferred to a 96-well plate for cultivation, whereas in condition 3 the cells mixed with the LunaGel™ were crosslinked and cultivated in a 96-well plate.

The results of the Tox-8 assay (see Figure 19) revealed similar metabolic activities in all three conditions tested, slightly more pronounced in condition 3. Compared to the day 0 reference corresponding to the metabolic activity of the cells in condition 2 after successful crosslinking of the hydrogels, it can be observed that the signals doubled within the four days of cultivation meaning that the cells equally proliferated in all three conditions. Statistical analysis revealed no significant difference between the three conditions tested. However, a significant difference was detected for the day 0 reference and condition 3.

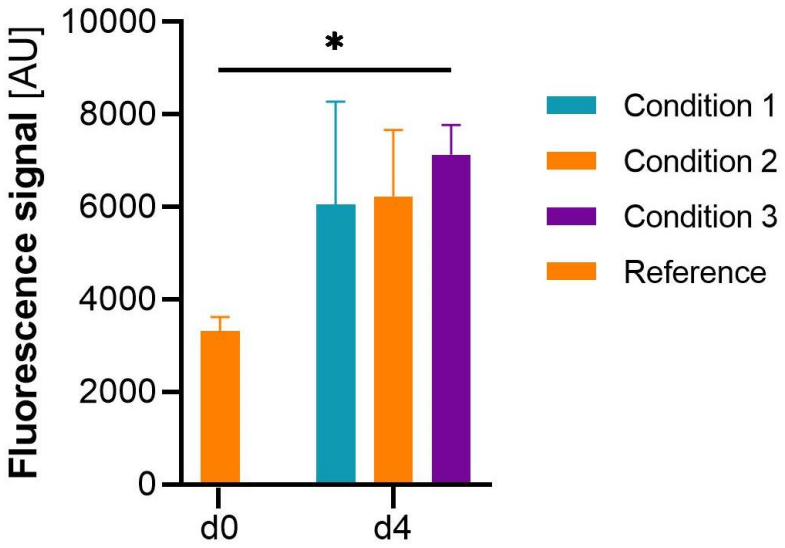

Figure 19: Assessment of the impact of the crosslinking procedure on cell growth by testing three different cultivation conditions. The measurement of the metabolic activity after four days of cultivation resulted in similar values for all three settings with a slightly higher signal observed for condition 3. In relation to the day 0 reference corresponding to the metabolic activity of the cells in condition 2 (bars therefore show the same coloring) after successful hydrogel crosslinking, it can be observed that the signals doubled within the four days of cultivation meaning that the cells equally proliferated in all three conditions (n=3, one-way ANOVA, significance determined using Tukey's multiple comparisons test, α= 0.05).

The findings of the live/dead staining are depicted in Figure 20. The calcein AM staining indicated the presence of elongated, spindle-shaped viable adMSC, appearing green in all three tested cultivation conditions. It can be observed that the immortalized adMSC K5 cells are most densely interconnected in condition 1 spreading through the hydrogel forming a 3D network of cells. In comparison, the cells in condition 2 and condition 3 also showed spreading through the hydrogel network over the cultivation period of four days, but it was less pronounced. In all three groups, a comparably small number of dead cells, stained by propidium iodide, could be detected after four days of cell expansion.

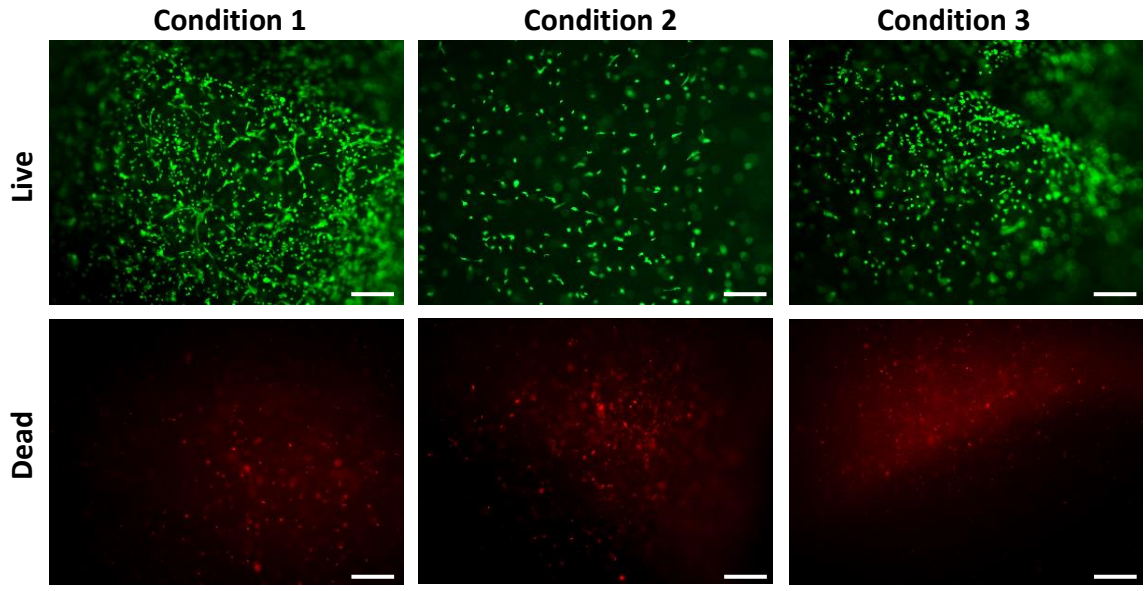

Figure 20: Live/dead staining of adMSC cultivated in three different conditions to evaluate the impact of the photocrosslinking procedure on cell growth, green - calcein AM: viable cells, red - propidium iodide: dead cells. A high number of living spindle-shaped cells can be observed in all three cultivation conditions whilst only a comparably small number of dead cells is visible. After four days of cell expansion, the adMSC seem to be most densely interconnected in condition 1 (scale bar = 200 µm).

As both assays revealed similar results for all three conditions tested, it could be concluded that the photocrosslinking procedure of the LunaGel™ in the scaffold holders made of silicon does not affect cell growth. Consequently, this procedure is not the reason for the cells dying during the cultivation in the Oli-UP 3D cell culture system. Otherwise, the cell metabolic activities as well as cell growth should have been perceptibly affected in the first two conditions tested.

3.5 3D cultivation in PEEK cultivation chambers

After consultation with the manufacturer of the Oli-UP 3D cell culture system, new 5-well cultivation chambers made of the chemically inert material PEEK were provided ensuring that the material does not interfere with cell growth during the 3D expansion of adMSCs. For the cultivation in the gelatinemethyalcyrol-based LunaGel™, the immortalized cell line adMSC K5 was grown under ambient oxygen conditions in the Oli-UP 3D cell culture system using the new chambers followed by staining the cells with calcein AM and propidium iodide for assessment of cell proliferation.

The results of the live/dead staining depicted in Figure 21, indicated a high number of living cells, stained by calcein AM, on day 0. The viable single cells are round-shaped being evenly distributed in the hydrogels. On the contrary, the propidium iodide staining revealed only a small number of dead cells. However, only very few living cells were visible on day 4 and day 7, whilst the propidium iodide staining resulted in an elevated number of dead cells.

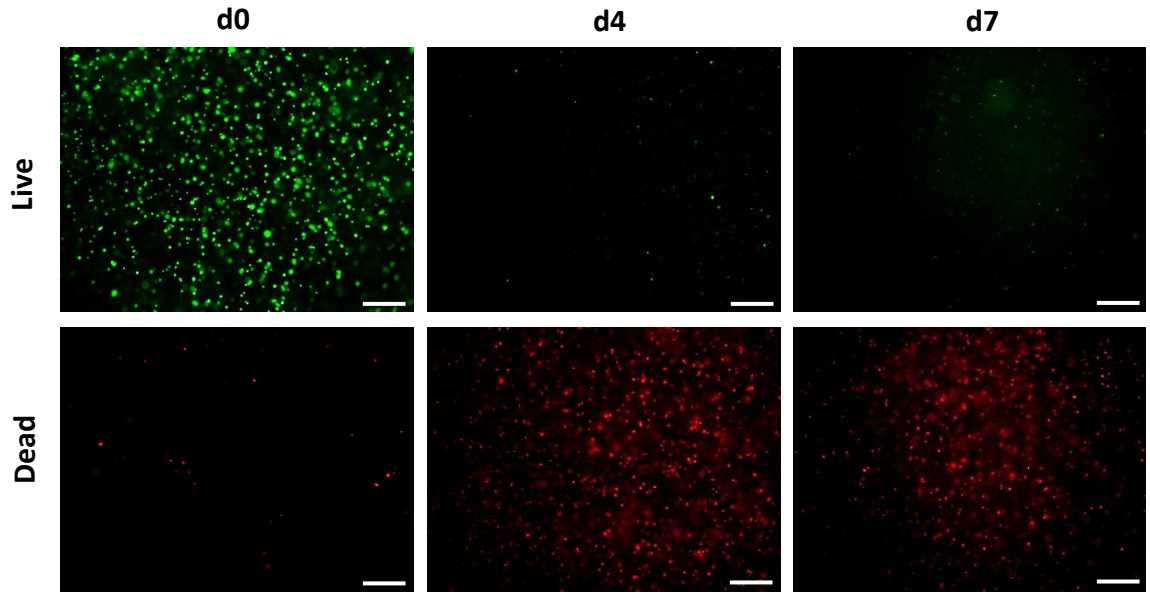

Figure 21: Live/dead staining of adMSC expanded in PEEK cultivation chambers, green - calcein AM: viable cells, red - propidium iodide: dead cells. A high number of round-shaped evenly distributed viable cells can be observed on day 0, whilst the propidium iodide staining revealed only a minor number of dead cells. Nevertheless, only very few living cells were visible on day 4 and day 7 whereas elevated numbers of dead cells were detected meaning that almost all adMSC died throughout the cultivation period of seven days (scale bar = 200 µm).

With the new PEEK cultivation chambers, similar results as in section 3.3 were obtained with the stem cells having died during the 3D hydrogel expansion in the Oli-UP cell culture system. It would have been expected that the adMSC proliferate within the seven days of cultivation, spreading through the hydrogel, which provides a convenient microenvironment for cell adhesion. The stem cells appear in a round shape on day 0 as those images were taken directly after embedding the cells in hydrogel. However, the cells should have adapted their typical spindle-shaped morphology, while building up their own ECM in the hydrogel throughout the cultivation. Instead, a major part of the initially seeded cells died during the 3D hydrogel expansion in the Oli-UP cell culture system.

It can be concluded that there are serious technical problems with the Oli-UP 3D cultivation system that could not be solved together with the manufacturer LifeTaq Analytics within the scope of this master project. There are presumably problems with the gas and nutrient supply

of the stem cells during the 3D cultivation as the exchange surface is probably too small and the cultivation chambers are possibly too deep for the substances to reach the cells.

3.6 6-well plate cultivation

For the validation of the growth behavior of primary adMSC as well as of the immortalized cell line adMSC K5 during 3D hydrogel expansion, the cells were cultured in 6-well plates as the technical problems with the 3D cultivation in the Oli-UP cell culture system could not be solved together with the manufacturer. In this alternative setup, both cell types were grown under normoxic and hypoxic oxygen conditions followed by measuring the metabolic activity and staining the cells with calcein AM and propidium iodide.

The values of the Tox-8 assay presented in Figure 22 are blanked and normalized to day 0 samples as the metabolic activities obtained for the first measurement on day 0 were quite diverse within the four groups observed. The bar chart shows the metabolic activities revealed for the two different cell types cultured under normoxic and hypoxic conditions. It is visible that the signals rise with the course of cultivation in all four groups meaning that the cells proliferated in all conditions within the seven days. With the primary adMSC, increased proliferation and thus an elevated metabolic activity can be observed under hypoxic conditions. In comparison, the adMSC K5 display a higher metabolic activity under ambient oxygen concentrations of 21 %. It must be mentioned that the absolute fluorescence values have generally been way higher for the cultivation under 5 % oxygen, but when normalized to day 0 samples, the values are higher for the normal oxygen conditions. The highest metabolic activity has generally been measured for the immortalized cell line adMSC K5 meaning that those cells proliferated faster compared to the primary adMSC. Statistical analysis revealed significant differences in the metabolic activities between the different cell types cultured under ambient and hypoxic oxygen concentrations. The individual significances are indicated in Figure 22.

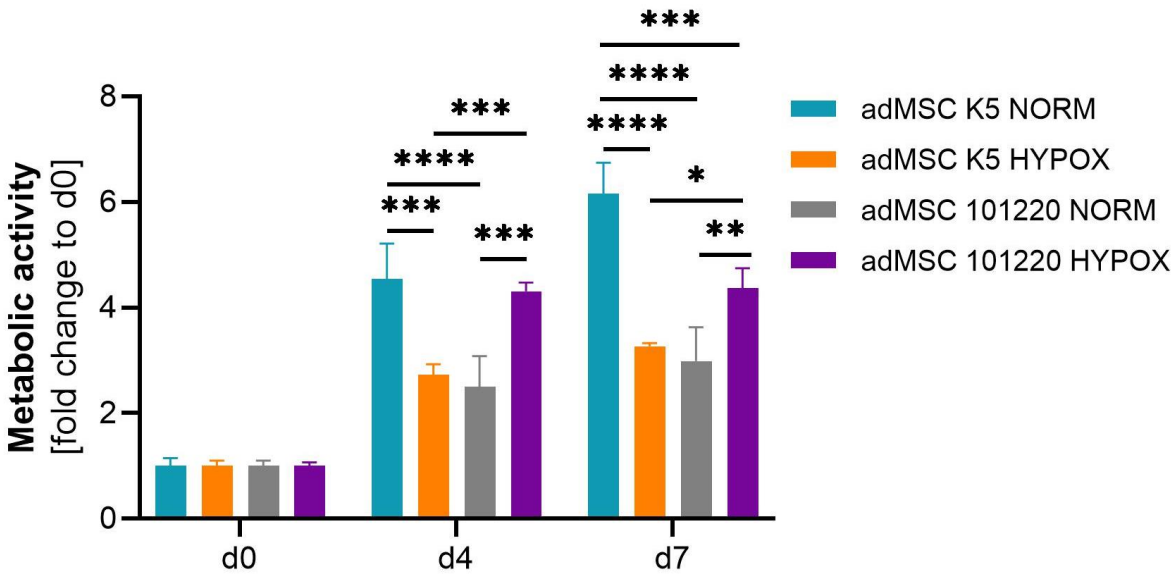

Figure 22: 3D expansion of primary adMSC and the immortalized cell line adMSC K5 during 6-well plate cultivation. The measurement of the metabolic activities revealed rising signals in all four groups throughout cultivation. For the primary cells, higher values can be observed under hypoxic conditions, whereas for the adMSC K5 the metabolic activity is higher under ambient oxygen conditions. The values presented are blanked and normalized to day 0 samples (n=5, one-way ANOVA, significance determined using Tukey's multiple comparisons test, α= 0.05).

The results of the calcein AM propidium iodide staining (see Figure 23) also show that the cells proliferated within the seven days of cultivation in all four conditions observed. On day 0 living single cells in a round shape being evenly distributed in the hydrogels can be observed in all four groups. On day 4 and especially on day 7 the adMSC appear in an elongated spindle-shaped form having spread through the hydrogel. The cells could establish extensive cell-cell contacts forming a 3D cellular network. On day 4, no distinct differences are visible between the individual groups. However, on day 7 the two hydrogels cultured under hypoxic conditions appear to be most densely overgrown, even more pronounced with the adMSC K5 cultured under hypoxic conditions. In both groups, the cells populate the entire hydrogel in all three dimensions after seven days of cultivation. The number of dead cells, stained by propidium iodide, increased throughout the cultivation period in all four groups. Nevertheless, the number of dead cells was comparably small in relation to the number of proliferating living cells in all conditions observed.

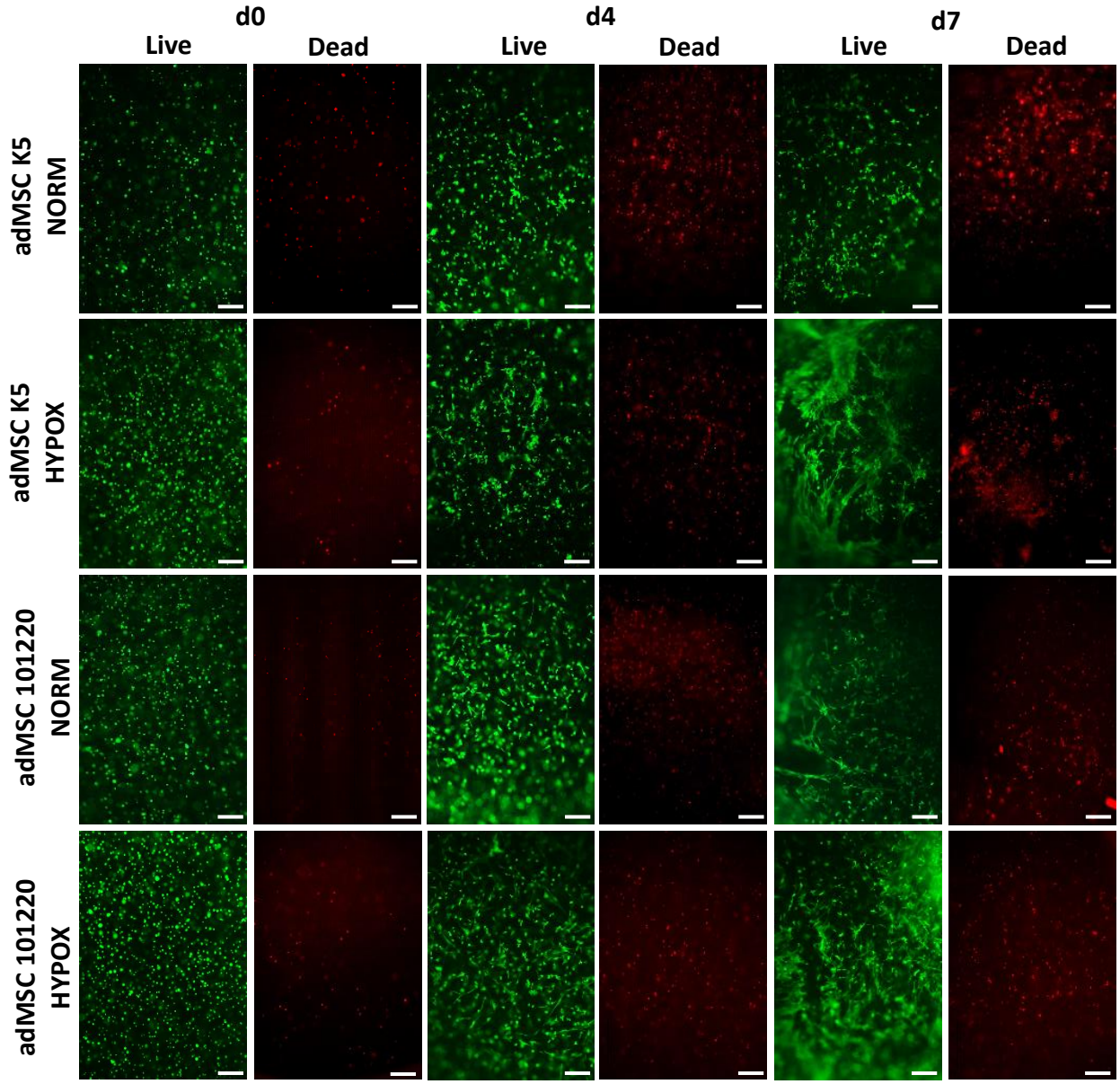

Figure 23: Live/dead staining of primary adMSC and the immortalized cell line adMSC K5 cultured at two different oxygen conditions in 6-well plates, green - calcein AM: viable cells, red - propidium iodide: dead cells. On day 0 round-shaped single cells that are evenly distributed in the hydrogels can be observed in all four groups, whilst on day 4 and especially on day 7, the adMSC appear in an elongated spindle-shaped form having spread through the hydrogels. On day 7, the two hydrogels cultured under hypoxic conditions appear to be most densely overgrown, even more pronounced with the adMSC K5 cultured under hypoxic conditions. The number of dead cells, stained by propidium iodide, increased throughout the cultivation period in all four groups being still comparatively small (scale bar = 200 µm).

For the evaluation of the growth behavior of the different adMSC types, it was expected that the cells proliferate over the cultivation period resulting in rising metabolic activities within the seven days. This was exactly what was observed in all 4 groups. Furthermore, increased proliferation is usually observed under hypoxic conditions, which could be detected for the primary adMSC in the Tox-8 assay. However, for the immortalized cell line higher metabolic activities were observed for the cells cultured under normoxia when normalizing the values

to day 0 samples. When looking at the absolute fluorescence values, the data were way higher for the adMSC K5 cultured under hypoxic oxygen conditions. The results of the live/dead staining give a different impression as both cell types spread most severely when cultured at 5 % oxygen with the hydrogel of the adMSC K5 appearing to be most densely overgrown. A possible explanation for these findings is that for the adMSC K5 cultured at ambient oxygen concentrations, a smaller cell number was erroneously seeded on day 0 as cell counting via hemocytometer is not that exact. When looking at the results of the calcein AM staining of the day 0 samples, there seem to be fewer cells in the microscopy image taken for this group compared to the three other groups. Consequently, the metabolic activity measured for the cell line cultured at 21 % oxygen is higher in relation to the other groups when comparing the values to day 0 samples.

It could be identified that the primary cells adMSC 101220 as well as the immortalized cell line adMSC K5 are generally rather similar in their morphology and growth behavior. However, the cell line is less sensitive when being cultured and seems to proliferate faster displaying an enhanced migration potential compared to the non-immortalized primary adMSC even if it is not fully clear from the Tox-8 data obtained. These findings are consistent with the observations reported by Burk et al. [26]. Moreover, it could be shown that both cell types display enhanced proliferation during the 3D expansion under hypoxic oxygen concentrations reflecting the natural in vivo environment of adMSC. It could be demonstrated that the oxygen concentration is a crucial microenvironmental parameter for the physiologic cultivation of adMSC significantly affecting cell proliferation during cell expansion.

3.7 Hydrogel expansion

As the future perspective is to fully automate the cultivation of cells in the Oli-UP cell culture system, the continuous 3D hydrogel expansion of cells was evaluated by passaging the immortalized cell line adMSC K5 two times while being embedded in LunaGel™. The feasibility of this passaging procedure was checked by measuring the metabolic activity followed by staining the cells with calcein AM and propidium iodide.

The Tox-8 data depicted in Figure 24 are blank corrected. On day 4 and day 9, two bars can be seen, with the blue bars generally corresponding to the metabolic activities before passaging and the grey bars representing the metabolic activities after passaging. There is only one bar visible for day 0 and day 14 as the adMSC have not been passaged on those days. The metabolic activity raised between day 0 and day 4 meaning that the cells proliferated within this cultivation period. The value drops to around one third after passaging on day 4 what fits the dilution factor of 1:3.5. However, there is only a slight increase in metabolic activity between day 4 and day 9, while the fluorescence signal drops sharply after passaging on day 9 being hardly detectable. On day 14 only a few metabolic active cells were left with the value being twice as high as on day 9 after passaging.

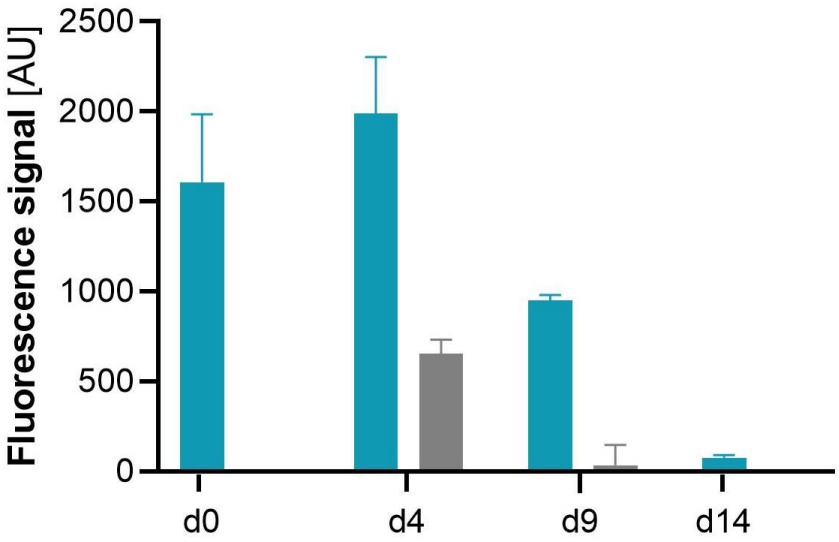

Figure 24: Evaluation of continuous 3D hydrogel expansion of adMSC. The cells were passaged two times while being embedded in LunaGel™ with the blue bars generally corresponding to the metabolic activities before passaging and the grey bars representing the metabolic activities after passaging. The metabolic activity increased between day 0 and day 4 signifying cell proliferation, while the value drops to around one third after passaging on day 4 fitting the dilution factor of 1:3.5. However, there is only a slight increase in metabolic activity between day 4 and day 9, whereas it drops sharply after passaging on day 9 being hardly detectable. The measurement of the fluorescence signal on day 14 revealed a value being twice as high as on day 9 after passaging, still being rather low. The values presented are blanked.

In contrast to the measurement of the metabolic activity, the calcein AM propidium iodide staining (see Figure 25) was additionally conducted on day 21 of the experiment. On day 4 and day 9 two microscopy images are visible for each staining, whereas the upper one corresponds to the staining performed before passaging and the lower one depicts the stained cells after the passaging procedure. For day 0, day 14, and day 21 of the cultivation, only one microscopy image per staining is presented as the cells have not been passaged on these days. Cell proliferation can be observed between day 0 and day 4. While on day 0 single

cells in a round shape are visible, the adMSC appear in an elongated spindle-shaped form having spread through the hydrogel after four days of cultivation. After passaging the cells on day 4, the number of living cells decreased to around one third. The cells are no longer evenly distributed and seem to receive the cell-cell contacts forming a 3D cellular network beyond the homogenization procedure as the adMSC appear in cell aggregates. However, it is visible that the cells did not proliferate much until day 9 with the adMSC having not spread through the hydrogel. After the passaging procedure on day 9, only a few living cells were left that did not further proliferate when being cultured for another few days. The number of living cells stayed constant until the experiment was finally ended on day 21 of cultivation. The number of dead cells, stained by propidium iodide, was generally small and did not increase throughout the cultivation period of 21 days.

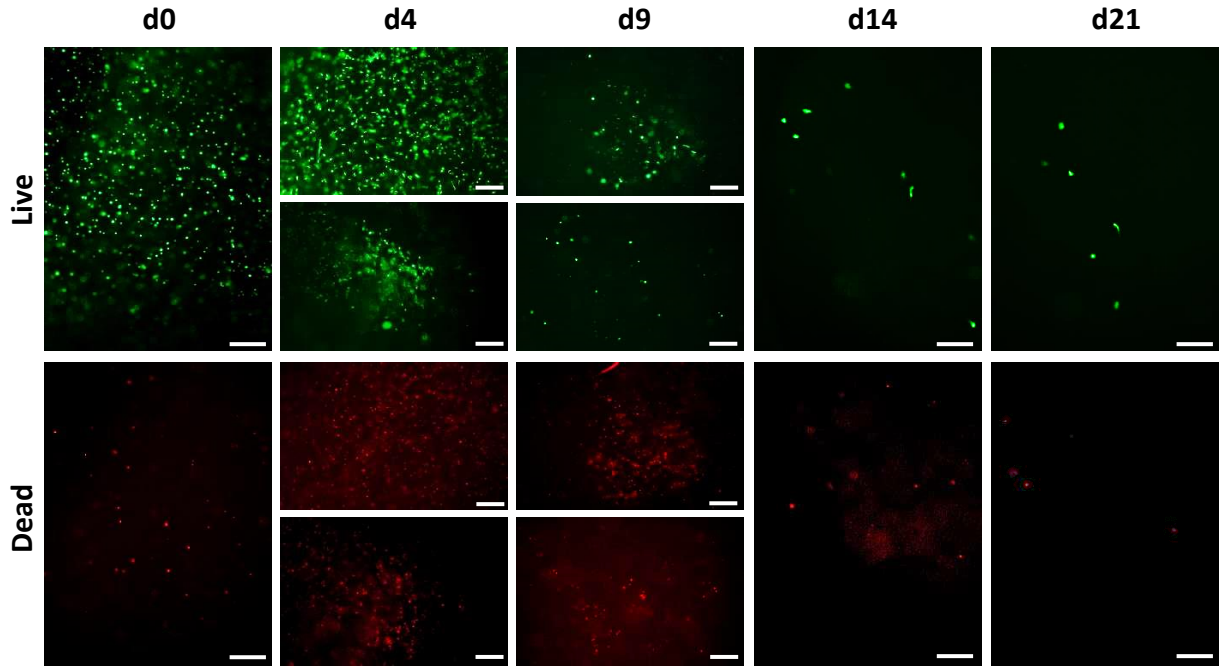

Figure 25: Live/dead staining revealed during continuous 3D hydrogel expansion of adMSC K5, green - calcein AM: viable cells, red - propidium iodide: dead cells. On day 4 and day 9 two microscopy images are visible for each staining, whereas the upper one corresponds to the staining performed before passaging and the lower one depicts the stained cells after the passaging procedure. On day 0 round-shaped single cells that are evenly distributed in the hydrogels can be observed, that appear in an elongated spindle-shaped form having spread through the hydrogel after four days of cultivation. After passaging the cells on day 4, the number of living cells decreased to around one third with the adMSCs appearing in cell aggregates. The cells did not proliferate much until day 9, whilst only a few living cells were left after passaging on that day that did not further proliferate when being cultured for another few days. The number of dead cells, stained by propidium iodide, was generally small and did not increase throughout the cultivation period of 21 days (scale bar = 200 µm).

The results of both analytical methods show that the hydrogel expansion was generally successful. Up to and including day 4 of cultivation, the results meet the expectations with the adMSC having proliferated and the cell number dropping to one third after the first passaging procedure. From this point on, the cells did not proliferate as it would have been expected until cell growth finally stalled. The experiment should be repeated with a few points to consider. One problem could have been that the time periods between the passages were probably too short. The adMSC most likely need elongated cultivation periods to regenerate after the quite stressful passaging procedures and to start proliferating again. A second point to address is that some cells were also lost during the passaging procedures as some hydrogel stuck to the mortar as well as to the wall of the 15 mL tube after homogenization. One last aspect that should definitely be considered would be to choose a smaller dilution factor. The factor of 1:3.5 was arbitrarily chosen for this initial trial with the ulterior motive to not waste material in case the 3D hydrogel expansion would not work. With a smaller dilution factor, the adMSC would probably restart growing faster after the passaging procedure as it is easier for them to find cell contacts. With those measures mentioned, it is likely that the hydrogel expansion will result in more promising outcomes when repeating the experiment, which forms the fundamentals for the planned future automation of the 3D hydrogel expansion in the Oli-UP cell culture system.

4 Conclusion

Human MSC display various therapeutically relevant characteristics comprising a high self-renewal ability, a high proliferation capacity as well as a multi-lineage differentiation potential and can be easily obtained from donors in large numbers. Due to their individual properties, MSC are generally considered as promising candidates for cell-based therapies in the field of regenerative medicine. The field of research is rapidly increasing as the cells may provide therapeutic solutions for numerous human diseases utilizing their great tissue regeneration potential and immunomodulatory effects. Besides those clinical applications, the cells also show promising potential to be used for the construction of in vitro disease models, whereby MSC are seeded on 3D matrices for their generation. Such constructs are used for studying disease mechanisms, contribute to the understanding of the role and mechanisms of action of MSC in various regenerative processes, and can further be applied for drug screening, thus reducing animal testing. As those cells behave differently in artificial environments, it is important to mimic the native environment of the cells during expansion by implementing physiological conditions so that the results of scientific in vitro studies are predictable for subsequent in vivo studies.

The aim of this master thesis project was to establish a hydrogel-based 3D cell culture model with MSC in the so-called Oli-UP 3D cell culture system under physiological cultivation conditions. Within the scope of this thesis, the growth behavior of primary adMSC and the immortalized cell line adMSC K5 should have been investigated and validated during the 3D expansion in the Oli-UP cell culture system under normoxic (21 % O_2) and hypoxic (5 % O_2) conditions by using suitable tests. Thus, the metabolic activity was determined followed by staining the cells with calcein AM and propidium iodide. However, it had to be ascertained that there are serious technical problems with the Oli-UP 3D cultivation system that could not be solved together with the manufacturer LifeTaq Analytics within the scope of this master project. Therefore, an alternative setup was compiled. Instead of cultivating the cells embedded in LunaGel™ in a vertical way in the Oli-UP cultivation chambers, they were expanded horizontally in 6-well plates. It could be demonstrated that both cell types display enhanced proliferation when being expanded under hypoxic oxygen concentrations compared to normoxic conditions. Thus, it could be proven that the oxygen concentration is

a crucial microenvironmental parameter for the physiologic cultivation of adMSC significantly affecting the cell proliferation during cell expansion. It could further be identified that the primary adMSC, as well as the immortalized cell line adMSC K5, are generally rather similar in their morphology and growth behavior. However, the cell line is less sensitive when being cultured and proliferates faster displaying an enhanced migration potential compared to the non-immortalized primary adMSC.

As the focus of the whole project is on the full automation of the 3D cell culture model, the feasibility of the continuous 3D expansion of cells while being embedded in hydrogel was additionally evaluated. Therefore, the immortalized cell line adMSC K5 was passaged two times while being embedded in LunaGel™ with the practicability of this procedure being investigated by measuring the metabolic activity followed by staining the cells with calcein AM and propidium iodide. The preliminary trial resulted in promising outcomes with the hydrogel expansion being generally successful representing the first important step towards the achievement of a continuous 3D expansion. However, the experiment should be repeated with a few points to consider as cell growth finally stalled. Besides elongated cultivation periods, a smaller dilution factor would be advisable. With those measures, it is likely that the results of the hydrogel expansion will be improved, whereat the experiment forms the fundamentals for the planned future automation of the 3D hydrogel expansion in the Oli-UP cell culture system.

Summing up, for the successful establishment of the in vitro model in the Oli-UP 3D cell cultivation system, extensive effort needs to be raised to refine the device. It would be advisable to increase the exchange surface as there are presumably problems with the gas and nutrient supply of the cells during the 3D cell expansion. Moreover, the design of the cultivation chambers should be rethought as the chambers are possibly too deep for the cells to be supplied appropriately. However, ongoing research will hopefully help to successfully overcome these current challenges as the in vitro model has promising prospects to be effectively applied in scientific research in the future, contributing to the understanding of the role and mechanisms of action of MSCs in various regenerative processes, while additionally facilitating the testing of new treatment options without having to sacrifice animals.

5 References

[1] L. Mazini, L. Rochette, M. Amine, and G. Malka, “Regenerative capacity of adipose derived stem cells (ADSCs), comparison with mesenchymal stem cells (MSCs),” *Int. J. Mol. Sci.*, vol. 20, no. 2523, pp. 1–30, 2019.

[2] J. Dulak, K. Szade, A. Szade, W. Nowak, and A. Józkowicz, “Adult stem cells: Hopes and hypes of regenerative medicine,” *Acta Biochim. Pol.*, vol. 62, no. 3, pp. 329–337, 2015.

[3] Z. Si *et al.*, “Adipose-derived stem cells: Sources, potency, and implications for regenerative therapies,” *Biomed. Pharmacother.*, vol. 114, no. June, 2019.

[4] E. Keung, P. Nelson, and C. Conrad, “Concise Review: Adipose-Derived Stem Cells as a Novel Tool for Future Regenerative Medicine,” *Stem Cells*, vol. 30, pp. 804–810, 2013.

[5] D. Mushahary, A. Spittler, C. Kasper, V. Weber, and V. Charwat, “Isolation, cultivation, and characterization of human mesenchymal stem cells,” *Cytom. Part A*, vol. 93, no. 1, pp. 19–31, 2018.

[6] A. Bajek, N. Gurtowska, J. Olkowska, L. Kazmierski, M. Maj, and T. Drewa, “Adipose-Derived Stem Cells as a Tool in Cell-Based Therapies,” *Arch. Immunol. Ther. Exp. (Warsz).*, vol. 64, no. 6, pp. 443–454, 2016.

[7] B. A. Bunnell, “Adipose Tissue-Derived Mesenchymal Stem Cells,” *Cells*, vol. 10, no. 3422, 2021.

[8] H. Mizuno, “Adipose-derived Stem Cells for Tissue Repair and Regeneration: Ten Years of Research and a Literature Review,” *J. Nippon Med. Sch.*, vol. 76, no. 2, pp. 56–66, 2009.

[9] P. A. Zuk *et al.*, “Human Adipose Tissue Is a Source of Multipotent Stem Cells,” *Mol. Biol. Cell*, vol. 13, pp. 4279–4295, 2002.

[10] C. Chavez-Munoz, K. T. Nguyen, W. Xu, S. J. Hong, T. A. Mustoe, and R. D. Galiano, “Transdifferentiation of adipose-derived stem cells into keratinocyte-like cells: Engineering a stratified epidermis,” *PLoS One*, vol. 8, no. 12, 2013.

[11] M. J. Seo, S. Y. Suh, Y. C. Bae, and J. S. Jung, “Differentiation of human adipose stromal cells into hepatic lineage in vitro and in vivo,” *Biochem. Biophys. Res. Commun.*, vol. 328, no. 1, pp. 258–264, 2005.

[12] U. G. Thakkar, H. L. Trivedi, A. V. Vanikar, and S. D. Dave, “Insulin-secreting adipose-derived mesenchymal stromal cells with bone marrow-derived hematopoietic stem cells from autologous and allogenic sources for type 1 diabetes mellitus,” *Cytotherapy*, vol. 17, no. 7, pp. 940–947, 2015.

[13] L. Bacakova *et al.*, “Stem cells: their source, potency and use in regenerative therapies with focus on adipose-derived stem cells – a review,” *Biotechnol. Adv.*, vol. 36, no. 4, pp. 1111–1126, 2018.

[14] H. Salehi, N. Amirpour, A. Niapour, and S. Razavi, “An Overview of Neural Differentiation Potential of Human Adipose Derived Stem Cells,” *Stem Cell Rev. Reports*, vol. 12, no. 1, pp. 26–41, 2016.

[15] D. Egger, A. Lavrentieva, P. Kugelmeier, and C. Kasper, “Physiologic isolation and expansion of human mesenchymal stem/stromal cells for manufacturing of cell-based therapy products,” *Eng. Life Sci.*, vol. 22, no. 3–4, pp. 361–372, 2022.

[16] Z. Zhang, M. J. Gupte, and P. X. Ma, “Biomaterials and Stem Cells for Tissue Engineering,” *Expert Opin. Biol. Ther.*, vol. 13, no. 4, pp. 527–540, 2013.

[17] R. Alvites, M. Branquinho, A. C. Sousa, B. Lopes, P. Sousa, and A. C. Maurício, “Mesenchymal Stem/Stromal Cells and Their Paracrine Activity—Immunomodulation Mechanisms and How to Influence the Therapeutic Potential,” *Pharmaceutics*, vol. 14, no. 2, 2022.

[18] A. J. Salgado, R. L. Reis, N. Sousa, and J. M. Gimble, “Adipose Tissue Derived Stem Cells Secretome: Soluble Factors and Their Roles in Regenerative Medicine,” *Curr. Stem Cell Res. Ther.*, vol. 5, no. 2, pp. 103–110, 2010.

[19] K. Mesimäki *et al.*, “Novel maxillary reconstruction with ectopic bone formation by GMP adipose stem cells,” *Int. J. Oral Maxillofac. Surg.*, vol. 38, no. 3, pp. 201–209, 2009.

[20] H. N. Zhang, L. Li, P. Leng, Y. Z. Wang, and C. Y. Lü, “Uninduced adipose-derived stem cells repair the defect of full-thickness hyaline cartilage,” *Chinese J. Traumatol.*, vol. 12, no. 2, pp. 92–97, 2009.

[21] S. J. Hong *et al.*, “Topically Delivered Adipose Derived Stem Cells Show an Activated-Fibroblast Phenotype and Enhance Granulation Tissue Formation in Skin Wounds,” *PLoS One*, vol. 8, no. 1, p. e55640, 2013.

[22] R. S. Waterman, S. L. Tomchuck, S. L. Henkle, and A. M. Betancourt, “A new mesenchymal stem cell (MSC) paradigm: Polarization into a pro-inflammatory MSC1 or an immunosuppressive MSC2 phenotype,” *PLoS One*, vol. 5, no. 4, p. e10088, 2010.

[23] National Library of Medicine, “ClinicalTrials.gov.” [Online]. Available: https://clinicaltrials.gov/.

[24] J. A. Burdick, R. L. Mauck, and S. Gerecht, “To Serve and Protect: Hydrogels to Improve Stem Cell-Based Therapies,” *Cell Stem Cell*, vol. 18, no. 1, pp. 13–15, 2016.

[25] M. E. Wechsler, V. V. Rao, A. N. Borelli, and K. S. Anseth, “Engineering the MSC Secretome: A Hydrogel Focused Approach,” *Adv. Healthc. Mater.*, vol. 10, no. 7, pp. 1–32, 2021.

[26] J. Burk *et al.*, “Generation and characterization of a functional human adipose-derived multipotent mesenchymal stromal cell line,” *Biotechnol. Bioeng.*, vol. 116, no. 6, pp. 1417–1426, 2019.

[27] C. Lipps *et al.*, “Expansion of functional personalized cells with specific transgene combinations,” *Nat. Commun.*, vol. 9, no. 1, 2018.

[28] M. Miura *et al.*, “Accumulated Chromosomal Instability in Murine Bone Marrow Mesenchymal Stem Cells Leads to Malignant Transformation,” *Stem Cells*, vol. 24, no. 4, pp. 1095–1103, 2006.

[29] D. Hladik *et al.*, “Long-term culture of mesenchymal stem cells impairs ATM-dependent recognition of DNA breaks and increases genetic instability,” *Stem Cell Res. Ther.*, vol. 10, no. 1, pp. 1–12, 2019.

[30] D. Egger, I. Schwedhelm, J. Hansmann, and C. Kasper, “Hypoxic Three-Dimensional Scaffold-Free Aggregate Cultivation of Mesenchymal Stem Cells in a Stirred Tank Reactor,” *Bioengineering*, vol. 4, no. 47, 2017.

[31] C. Schmitz, E. Potekhina, V. V. Belousov, and A. Lavrentieva, “Hypoxia Onset in Mesenchymal Stem Cell Spheroids: Monitoring With Hypoxia Reporter Cells,” *Front. Bioeng. Biotechnol.*, vol. 9, no. February, 2021.

[32] B. M. Baker and C. S. Chen, “Deconstructing the third dimension-how 3D culture microenvironments alter cellular cues,” *J. Cell Sci.*, vol. 125, no. 13, pp. 3015–3024, 2012.

[33] Q. He *et al.*, “‘All-in-One’ Gel System for Whole Procedure of Stem-Cell Amplification and Tissue Engineering,” *Small*, vol. 16, no. 16, pp. 1–9, 2020.

[34] D. Rana and M. Ramalingam, “Enhanced proliferation of human bone marrow derived mesenchymal stem cells on tough hydrogel substrates,” *Mater. Sci. Eng. C*, vol. 76, pp. 1057–1065, 2017.

[35] Y. Bin Lee *et al.*, “Engineering spheroids potentiating cell-cell and cell-ECM interactions by self-assembly of stem cell microlayer,” *Biomaterials*, vol. 165, pp. 105–120, 2018.

[36] A. Lavrentieva *et al.*, “Gelatin-methacryloyl (GelMA) formulated with human platelet lysate supports mesenchymal stem cell proliferation and differentiation and enhances the hydrogel’s mechanical properties,” *Bioengineering*, vol. 6, no. 3, 2019.

[37] C. Kasper, D. Egger, and A. Lavrentieva, *Basic Concepts on 3D Cell Culture*. 2021.

[38] S. Yin and Y. Cao, “Hydrogels for Large-Scale Expansion of Stem Cells,” *Acta Biomater.*, vol. 128, pp. 1–20, 2021.

[39] S. Abdulghani and G. R. Mitchell, “Biomaterials for in situ tissue regeneration: A review,” *Biomolecules*, vol. 9, no. 11, 2019.

[40] D. Egger, C. Tripisciano, V. Weber, M. Dominici, and C. Kasper, “Dynamic cultivation of mesenchymal stem cell aggregates,” *Bioengineering*, vol. 5, no. 2, pp. 1–15, 2018.

[41] N.-C. Cheng, S.-Y. Chen, J.-R. Li, and T.-H. Young, “Short-Term Spheroid Formation Enhances the Regenerative Capacity of Adipose-Derived Stem Cells by Promoting Stemness, Angiogenesis, and Chemotaxis,” *Stem Cells Transl. Med.*, vol. 2, no. 8, pp. 584–594, 2013.

[42] T. J. Bartosh *et al.*, “Aggregation of human mesenchymal stromal cells (MSCs) into 3D spheroids enhances their antiinflammatory properties,” *Proc. Natl. Acad. Sci. U. S. A.*, vol. 107, no. 31, pp. 13724–13729, 2010.

[43] B. Follin, M. Juhl, S. Cohen, A. E. Perdersen, J. Kastrup, and A. Ekblond, “Increased Paracrine Immunomodulatory Potential of Mesenchymal Stromal Cells in Three-Dimensional Culture,” *Tissue Eng. - Part B*, vol. 22, no. 4, pp. 322–329, 2016.

[44] Q. Huang *et al.*, “Hydrogel scaffolds for differentiation of adipose-derived stem cells,” *Chem. Soc. Rev.*, vol. 46, no. 20, pp. 6255–6275, 2017.

[45] I. Pepelanova, K. Kruppa, T. Scheper, and A. Lavrentieva, “Gelatin-methacryloyl (GelMA) hydrogels with defined degree of functionalization as a versatile toolkit for 3D cell culture and extrusion bioprinting,” *Bioengineering*, vol. 5, no. 3, 2018.

[46] Gelomics Pty Ltd, “LunaGel^{TM} - Bovine Bone Gelatin - Photocrosslinkable Extracellular Matrix.” [Online]. Available: https://www.gelomics.com/product-page/bovine-bone-gelatin. [Acessed: 30.03.2022]

[47] M. Lönne, A. Lavrentieva, J. G. Walter, and C. Kasper, “Analysis of oxygen-dependent cytokine expression in human mesenchymal stem cells derived from umbilical cord,” *Cell Tissue Res.*, vol. 353, no. 1, pp. 117–122, 2013.

[48] M. Kukumberg *et al.*, “Hypoxia-induced amniotic fluid stem cell secretome augments cardiomyocyte proliferation and enhances cardioprotective effects under hypoxic-ischemic conditions,” *Sci. Rep.*, vol. 11, no. 1, pp. 1–15, 2021.

[49] C. Almeria *et al.*, “Hypoxia Conditioned Mesenchymal Stem Cell-Derived Extracellular Vesicles Induce Increased Vascular Tube Formation in vitro,” *Front. Bioeng. Biotechnol.*, vol. 7, pp. 1–12, 2019.

[50] W. L. Grayson, F. Zhao, B. Bunnell, and T. Ma, “Hypoxia enhances proliferation and tissue formation of human mesenchymal stem cells,” *Biochem. Biophys. Res. Commun.*, vol. 358, no. 3, pp. 948–953, 2007.

[51] Y. Yu *et al.*, “Effect of hypoxia on self-renewal capacity and differentiation in human tendon-derived stem cells,” *Med. Sci. Monit.*, vol. 23, pp. 1334–1339, 2017.

[52] K. E. Hawkins, T. V Sharp, and M. T. R, “The role of hypoxia in stem cell potency and differentiation,” *Regen. Med.*, vol. 8, no. 6, pp. 71–82, 2013.

[53] C. Schmitz *et al.*, “Live reporting for hypoxia: Hypoxia sensor–modified mesenchymal stem cells as in vitro reporters,” *Biotechnol. Bioeng.*, vol. 117, no. 11, pp. 3265–3276, 2020.

[54] J. Hansmann, F. Groeber, A. Kahlig, C. Kleinhans, and H. Walles, “Bioreactors in tissue engineering-principles, applications and commercial constraints,” *Biotechnol. J.*, vol. 8, no. 3, pp. 298–307, 2013.

[55] A. M. Leferink, Y. C. Chng, C. A. van Blitterswijk, and L. Moroni, “Distribution and viability of fetal and adult human bone marrow stromal cells in a biaxial rotating vessel bioreactor after seeding on polymeric 3D additive manufactured scaffolds,” *Front. Bioeng. Biotechnol.*, vol. 3, pp. 1–14, 2015.

[56] M. Haack-Sørensen *et al.*, “Culture expansion of adipose derived stromal cells. A closed automated Quantum Cell Expansion System compared with manual flask-based culture,” *J. Transl. Med.*, vol. 14, no. 1, pp. 1–11, 2016.

[57] G. Zhao *et al.*, “Large-scale expansion of Wharton’s jelly-derived mesenchymal stem cells on gelatin microbeads, with retention of self-renewal and multipotency characteristics and the capacity for enhancing skin wound healing,” *Stem Cell Res. Ther.*, vol. 6, no. 1, pp. 1–16, 2015.

[58] LifeTaq-Analytics GmbH, “GET STARTED IN 3D CELL CULTIVATION - Oli-UP.” [Online]. Available: https://lifetaq.com/resources/. [Acessed: 24.04.2022]

List of abbreviations

2D	Two-dimensional
3D	Three-dimensional
adMSC	Adipose derived mesenchymal stem cells
ATMPs	Advanced Therapies Medicinal Products
Calcein AM	Calcein acetoxymethyl
CD	Clusters of differentiation
DoF	Degree of functionalization
ECM	Extracellular matrix
EMA	European Medicine Agency
ESC	Embryonic stem cells
FDA	Food and Drug Administration
FGF-2	Fibroblast growth factor 2
GelMA	Gelatin-Methacryloyl
GM-CSF	Granulocyte/macrophage colony-stimulating factor
HGF	Hepatocyte growth factor
HLA-DR	Human leukocyte antigen-DR
hPL	Human platelet lysate
iPSC	Induced pluripotent stem cells
MSC	Mesenchymal stem cells
NGF	Nerve growth factor
PBT	Polybutylene terephthalate
PEEK	Polyetheretherketone
PEOT	Polyethylene oxide terephthalate

PI	Propidium Iodide
PTFE	Polytetrafluoroethylene
SDF-1α	Stromal-derived factor 1-alpha
TGF-β	Transforming growth factor beta
TLR	Toll-like receptor
UV	Ultraviolet
VEGF	Vascular endothelial growth factor

List of figures

List of tables

Appendix

A Lists of used materials

Table 3: List of used chemicals and solutions

Product	Manufacturer	Order number
Accutase® solution	Sigma-Aldrich	A6964-100ML
Agarose	Sigma-Aldrich	A9639-25G
Calcein AM	Thermo Fisher Scientific	C3099
DMSO	Sigma-Aldrich	D8418-100ML
Dulbecco´s Phosphate Buffered Saline	gibco®	21600-044
Ethanol ≥99.8%	Carl Roth	9065.1
Gentamycin solution	Sigma-Aldrich	G1272-100ML
Heparin	PL BioScience	PL-SUP-500
Human Platelet Lysate	PL BioScience	PE11011
MEM Alpha Medium	gibco®	12000-063
Propidium iodide	Sigma-Aldrich	81845-100MG
Sodium hydrogen carbonate	Sigma-Aldrich	401676-2.5KG
Trypan Blue solution	Sigma-Aldrich	T8154-100ML

Table 4: List of used equipment

Product	Manufacturer	Order number
Cell counting chamber, Neubauer improved	BRAND	-
Mortar	Carl Roth	-
Pipetboy	integra	1301765
Pipette Research® plus 0.1-2.5 µL	eppendorf	R20225G
Pipette Research® plus 2-20 µL	eppendorf	401006A
Pipette Research® plus 10-100 µL	eppendorf	362878Z
Pipette Research® plus 20-200 µL	eppendorf	402236A
Pipette Research® plus 100-1000 µL	eppendorf	K30171B

Table 5: List of used disposables

Product	Manufacturer	Order number
CELLSTAR® Serological pipette, sterile 5, 10, 25, 50 mL	greiner bio-one	606180, 607180, 760180, 768180
CELLSTAR® tubes 15, 50 mL	greiner bio-one	188271, 227261
CRYO.S™ tubes	greiner bio-one	122280
Glass pasteur pipettes	BRAND	747720
Multi®-SafeSeal®Tubes, 1.5 mL	Carl Roth	7080.1
Pipette tip 0.5-10 µL	greiner bio-one	771290
Pipette tip 2-200 µL	VWR	612-5755
Pipette tip 2-200 µL	BRAND	732008
Pipette tip 50-1000 µL	BRAND	732012
TC dish 150 mm	Sarstedt	83.3903
TC plate 6-, 24-, 48-, 96-well	Sarstedt	83.3920, 83.3922, 83.3923, 83.3924
TC flask T-75, T-175	Sarstedt	83.3911.002, 83.3912.002

Table 6: List of used kits

Product	Manufacturer	Order number
In Vitro Toxicology Assay Kit	Sigma-Aldrich	Tox8-1KT
LunaGel™ kit, Photocrosslinkable extracellular matrix	gelomics	SKU 0005
Oli-UP 3D cell culture kit	LifeTaq Analytics	-

Table 7: List of used media

Medium	Composition
α-MEM basal medium	10 g/L MEM alpha medium, 2.2 g/L sodium hydrogen carbonate
Cell culture medium	2.5% (v/v) human platelet lysate, 0.5% (v/v) gentamycin and 1 U/mL heparin in α-MEM

Table 8: List of used devices

Product	Manufacturer
Autoclave, Steam Sterilizer Type 500E	Thermo Scientific
Balance, AW-4202 and AW-224	Sartorius
Centrifuge 5702	eppendorf
Centrifuge, HERAEUS PICO 17	Thermo Scientific
Fluorescence microscope DMIL LED	Leica
Fluorescence microscope camera DFC420 C	Leica
Fluorescence microscope light EL6000	Leica
Incubator, HERACELL 240i	Thermo Scientific
Liquid nitrogen tank, Cryotherm	Biosafe® MD
Lunagel Crosslinker™	gelomics
Microscope (transmitted light), DMIL LED	Leica
Microscope camera ICC50 HD	Leica
Orbital shaker DOS-10M	ELMI
Plate reader, Infinite® M1000	Tecan
Sterile work bench, HERASAFE KS	Thermo Scientific
Vortex, Vortexgenie 2	Scientific Industries
Water bath	GFL

Table 9: List of used software

Software	Company	Version
BioRender	Open source	-
icontrol 1.6	Tecan	
ImageJ-win64	Open source	-
GraphPad Prism	GraphPad Software, Inc.	9.3.1
Leica Application Suite	Leica	3.4.0/4.6.1
Microsoft Excel	Microsoft	Office 365
Microsoft Word	Microsoft	Office 365

B Standard procedures

B.1 Thawing of cells

The respective cryo vial containing the cryopreserved cells was removed from the liquid nitrogen storage tank and swirled in a 37°C water bath until the cell suspension was completely thawed, but still cool. The cryo tube was sprayed with ethanol and placed in the flow hood. In the next step, 1 mL of room temperate α-MEM was added to the sample vial. After 2 minutes, the content was transferred to a 50 mL tube. The cryo tube was then rinsed with another 2 mL of α-MEM until the content was again added to the 50 mL tube. After 2 minutes, the cell suspension in the tube was filled up to 10 mL with α-MEM. The sample was then centrifuged at 300 x g for five minutes, the supernatant was removed with a sterile glass Pasteur pipette, and the pellet got flicked and resuspended in a defined volume cell culture medium. The volume of medium for resuspending depends on the size of the cell pellet.

The cell number of the cell suspension was then determined with a hemacytometer according to the protocol described in B.2. The cell suspension was then topped up to 15 mL with cell culture medium and transferred to a T-75 cell culture flask, which was incubated at 37°C and 5 % CO_2. On the next day, the medium was changed whereby 15 mL fresh cell culture medium was added to the flask.

B.2 Counting of cells

For the manual determination of the cell number of a cell suspension, a haemocytometer was used. This cell counting tool consists of two rectangular pits each possessing chambers of a defined volume, length, and depth. The perpendicular and horizontal lines which make up a grid, make it possible to count the number of cells in a defined area and volume in order to determine the cell number of the whole suspension. For the cell counting procedure, the haemocytometer was equipped with a glass cover slip which was placed on the surface of the counting chambers and fixed with ethanol. 20 µL cell suspension was then mixed with 20 µL trypan blue. This dye is used to assess cell viability as only dead cells are permeable, take up the dye, and appear blue. 10 µL of the suspension was then applied to the edge of the cover

slip of each chamber and sucked into the chambers by capillary action. A tally counter was then used to determine the number of living cells in eight large squares under the microscope. Figure 26 below shows the structure and dimensions of one chamber of the haemocytometer.

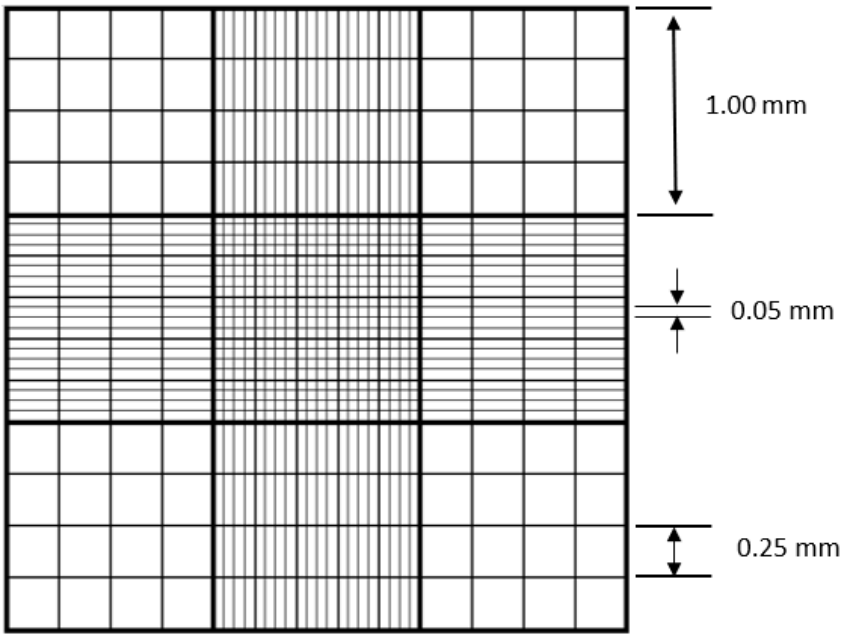

Figure 26: Structure of a haemocytometer counting chamber. The large squares have a side length of 1.00 mm, whereas the small squares are only 0.25 mm long. The depth of the chambers is 0.10 mm.

The total cell number of the cell suspension was then determined from the number of counted cells by using Equation 2.

$$\text{Cell number} = \frac{\text{counted cells}}{\text{number of large squares}} * \text{volume factor} * \text{dilution} * \text{volume} \qquad (2)$$

B.3 Passaging of cells

Cells were grown in T-flasks of different sizes until they reached a certain confluency. To avoid cell contact inhibition which leads to a reduction in doubling time, the adherent cells were usually passaged at a confluency of around 80 %. For the cell passaging procedure, the supernatant from the cells in the T-flask was discarded by sucking it off with a glass pasteur pipette. The cell layer was rinsed with prewarmed PBS to wash away media residues. The PBS was discarded and a defined volume of accutase was added and evenly distributed over the cell layer by tilting the flask. The volume of the enzyme added depended on the size of the T-flask. The T-flask was then incubated at 37°C and 5 % CO_2 for five minutes for cell detachment. Before stopping the enzymatic reaction with prewarmed cell culture medium by adding

approximately twice the volume that was previously added of the enzyme solution, it was checked under the microscope if the cells were detached and floating around. The surface of the flask was then rinsed several times with the added medium to remove all cells. The cell suspension was transferred to a 50 mL tube and centrifuged at 300 x g for five minutes. The supernatant was then sucked off with a glass pasteur pipette and the pellet was resuspended in a defined volume of cell culture medium that depended on the size of the pellet. To seed an appropriate number of cells, the cells were counted according to the procedure described in B.2. Finally, a T-flask of choice was filled with a defined volume of cell culture medium and a certain amount of cell suspension that depended on the desired seeding density was added. The flask was then put into the incubator for further cultivation. Table 10 below provides an overview of the commonly used volumes of medium and enzyme for the different sizes of T-flasks.

Table 10: Commonly used volumes for cell passaging

Flask	Volume of medium for cultivation [mL]	Volume of accutase [mL]	Volume of medium to stop enzyme reaction [mL]
T-75	15	1.5	4
T-175	25	3.5	8